1991ApJ...370..526C

THE ASTROPHYSICAL JOURNAL, 370:526–540, 1991 April 1
© 1991. The American Astronomical Society. All rights reserved. Printed in U.S.A.

A STUDY OF STAR FORMATION IN THE DISKS OF Sa GALAXIES

NELSON CALDWELL[1]
F. L. Whipple Observatory, Smithsonian Institution, P.O. Box 97, Amado, AZ 85645
ROBERT KENNICUTT
Steward Observatory, University of Arizona, Tucson, AZ 85721
ANDREW C. PHILLIPS
Department of Astronomy, University of Washington, Seattle, WA 98195
AND
ROBERT A. SCHOMMER[1]
Department of Physics and Astronomy, P.O. Box 849, Rutgers University, Piscataway, NJ 08854
Received 1990 March 26; accepted 1990 September 19

ABSTRACT

This paper presents an observational study of H II regions in seven Sa galaxies. The data consist of narrow-band Hα Fabry-Perot images and broad-band CCD images. The Fabry-Perot data allow us to measure luminosities of about 1000 H II regions in the Sa's, some as faint as 10^{36} ergs s^{-1}. The broad-band *UBV* measurements confirm expectations that the knots associated with the H II regions are very blue; the converse is also true. Luminosity functions of both H II regions and star clusters are computed. The H II region luminosity functions for Sa's are very steep, with few or no regions with $L(\mathrm{H}\alpha) > 10^{39}$ ergs s^{-1}. We discuss the probability that the initial mass function in Sa's is not significantly different from that in later type galaxies.

The total Hα luminosities for the galaxies are computed and used to derive the current star formation rates. We find that, in contrast to the later type galaxies, the current star formation rates in Sa disks are less than one-tenth of the average rate over the last 15 billion years. Because of those low rates, the formal depletion times of gas through star formation are longer than a Hubble time, despite the low gas densities. Thus, if the star formation in late-type galaxies takes on the character of that currently seen in the Sa's (once the gas density in the former galaxies drops below the appropriate threshold value), star formation in the late-type galaxies could continue for much longer than the usual estimate of 5 Gyr.

Subject headings: galaxies: stellar content — nebulae: H II regions — stars: formation

1. INTRODUCTION

The classification systems of disk galaxies proposed by Hubble (1936 and references therein), Lundmark (1926), and others drew astronomers' attention to the differences in appearances among those galaxies. For both the barred and unbarred galaxies, they identified as the paramount morphological features the relative dominance of the nuclear region (the bulge or spheroid) over the spiral disk, the tightness of the winding of the spiral arms, and the number and location of the condensations in the arms. The arm condensations revealed themselves to be sites of star formation, thus providing the first clue that the sequence of types from Sa to Sc (and on to Sd and Sm) was one of different star formation ability. The discovery that the bulge stars were primarily old further told us that the large bulge Sa galaxies had a different star formation history than the bulgeless late-type galaxies. The existence of S0 galaxies, ones which have bulges and disks without any spiral arms and thus apparently no current star formation, further confirmed convictions that somehow star formation had proceeded differently in different galaxies, and that these differences led to the current variety of morphologies.

The integral of the star formation history can be easily determined, and has formed the basis for several important papers in the study of galaxy evolution (Searle, Sargent, & Bagnuolo 1973; Larson & Tinsley 1978). The study of current star formation requires more detailed measurements, either of the emission lines found in H II regions or the ultraviolet continuum, but it has also been the subject of noteworthy papers on late-type galaxies, those with prodigous current star formation rates. The study of star formation where it is rare, in the Sa and S0 galaxies, has been neglected to a degree explainable only by its intrinsic difficulty. This paper attempts to rectify that shortcoming.

A brief foray into current star formation in early-type galaxies took place in the mid-1970s. Both van den Bergh (1976) and Kormendy (1977) reported detecting no Hα in the knots seen in two early spiral galaxies (NGC 4594, an Sa galaxy known better by the name Sombrero, and NGC 2841, an Sb galaxy). They speculated that the initial mass function (IMF) for star formation in those galaxies is truncated at the massive end so that no stars massive enough, and thus hot enough, to provide ionizing photons are being formed. The edge-on Sombrero galaxy has a prominent dust lane in the disk, and since the elements that constitute interstellar dust are made in massive stars, a small paradox was created by this belief, as van den Bergh himself pointed out. Schweizer (1978), Hodge & Kennicutt (1983), and Kennicutt (1988) later showed that H II regions did exist in those particular galaxies, and thus some stars more massive than 10 $M_\odot$ are indeed present, but since Schweizer only reported the detection of two H II regions in the Sombrero, it might be still believed that many of the rest of the blue knots seen in that galaxy and other Sa's are not H II regions. We review this controversy here, not because we

[1] Visiting Astronomer, Cerro Tololo Inter-American Observatory, operated by AURA, Inc., under contract from the National Science Foundation.

© American Astronomical Society • Provided by the NASA Astrophysics Data System

1991ApJ...370..526C

believe it is still viable but because it was in part responsible for the birth of this project some years ago. The data reported in this paper show that the Sombrero and other Sa galaxies are resplendent with H II regions, thus casting much doubt on the possibility that the IMF varies with any significance among galaxies of different Hubble type.

In addition to reporting the finding of several hundred H II regions in seven Sa galaxies, this paper compares the luminosity functions of the H II regions in Sa's with those of the later type galaxies, presents data on the associated star clusters, and finally calculates star formation rates.

2. DETECTION OF H II REGIONS IN Sa GALAXIES

2.1. *Selection of Galaxies*

For the stated reasons of historical interest, the first galaxy we studied was the Sombrero. The results from that study, included here, encouraged us to obtain a larger sample, and also made us aware that the Sombrero, being edge-on, was in fact a difficult galaxy to work on. For the subsequent observing runs, we chose six other galaxies to study that satisfied the general criteria of being (1) more face-on than edge-on, (2) at a distance of 10–30 Mpc, so that a large portion of the galaxy could be observed with the small-format detectors available, (3) classified as Sa or SBa in the Revised Shapley-Ames Catalog (Sandage & Tammann 1987, hereafter RSA), but (4) not strongly barred. For comparison, we included one Sab and one Sc galaxy as well, chosen to satisfy the same criteria. With the exception of NGC 4594, the chosen Sa galaxies have luminosities within 1 mag of the mean absolute magnitude of all of the Sa's found in the RSA. None are in dense clusters, nor even in tight groups. Sa galaxies in the RSA seem to cover a wide range of bulge/disk ratios and spiral arm resolution; we believe that our sample fairly represents that range of properties. Table 1 identifies the galaxies, along with their vital statistics and the observation dates.

The distances were obtained assuming $H_0 = 75$ km s^{-1} Mpc^{-1} and a linear infall model to the Virgo Cluster with a Local Group infall velocity of 300 km s^{-1}. The magnitudes and velocities were taken from the RSA or from this study.

These galaxies were inspected on the SERC IIIa-J sky survey films and IIa-O plates taken with the du Pont telescope and found to be for the most part rather smooth armed, with only a few knots showing up in the Sa's. NGC 1079 in particular was very smooth armed. Based on the appearance of these galaxies on plates, we therefore expected to detect only a few H II regions in the Sa's, if anything. CCD frames of the galaxies taken with large telescopes (Fig. 8; see below) do show a large number of knots, which we concentrated on in the Fabry-Perot work.

2.2. *Fabry-Perot Observations*

From private discussions with astronomers who had used low-resolution spectra or narrow-band filters to detect emission lines in early-type galaxies (with limited success), we surmised that a more powerful technique would be needed to detect ionized gas emission from what we expected to be low-luminosity H II regions in galaxies as far away as 30 Mpc. The Rutgers Imaging Fabry-Perot (Schommer et al. 1988) has been shown to be a superior instrument for detecting weak emission when used at the Cassegrain focus of a 4 m telescope, with a 3 σ detection limit of about 1×10^{-18} ergs s^{-1} cm^{-2} Å^{-1} in a 2.4 Å FWHM bandpass exposure of 15 minute duration in a moonless sky. This instrument was scheduled for our use on the CTIO 4 m telescope for three separate observing runs beginning in 1985. For the first run, during which only the Sombrero was observed, a GEC CCD was used as the detector. This resulted in a scale of 0".52 pixel^{-1} and a circular field of diameter 3'. For the later runs, a TI CCD was used as the detector, giving 0".71 pixel^{-1} and of course the same field size. It was with the TI detector that we obtained the quoted flux limits. The effective readout noise, including a charge-transfer improving preflash, was about 15 e^-. We used 80 Å bandpass filters to separate the orders, thus giving us 2.4 Å bandpass frames with a falloff in wavelength of 6 Å from the field center to the edge. The filters were chosen to pass the redshifted Hα line for the particular galaxy being observed.

All of the galaxies were 2 to 3 times larger than the CCD field, so the telescope was set to a position in the galaxy where the disks of the galaxies more or less filled the field. All exposures at the 4 m telescope were 15 minutes long, in a sky that had no more than a quarter Moon. The occasional presence of moonlight decreased the detection limit to about 3×10^{-18} ergs s^{-1} cm^{-2} Å^{-1}. The procedure was to take the first exposure at the expected redshifted wavelength of Hα. If no emission was seen, the Fabry-Perot was retuned to a wavelength one bandpass away and another exposure was taken (the rotation of the galaxy contributes a shift of 2–4 Å; we usually did not know the sense of the rotation before the observations). Once the right wavelength was found in this manner, further exposures were taken around that to ensure that the continuum was also reached for every detected emission region. Typically, six or seven exposures spaced at half the bandpass were all that were needed to get full spectral coverage of all of the emission-line regions found in the field. The seeing ranged from 1".3 to 2".3 FWHM during the observations. A total of about

TABLE 1

PROGRAM GALAXIES

Galaxy	Type	M_B	Velocity	Distance	Observation Date	Number of Fields	Fraction Observed
NGC 1079	Sa	−20.1	2165	29.4	1986 Oct	1	0.27
NGC 1291	SBa	−20.6	689	10.1	1988 Sep	1	0.07
NGC 1302	Sa	−20.2	1599	22.3	1986 Oct	2	0.66
NGC 1371	Sa	−19.8	1350	19.1	1986 Oct	2	0.36
NGC 1398	Sab	−20.9	1404	19.9	1986 Oct	1	0.17
NGC 4594	Sa+/Sb−	−22.3	1076	16.0	1985 Jun	2	0.60
NGC 7410	SBa	−20.5	1681	22.7	1986 Oct	1	0.55
NGC 7689	Sc	−19.6	1681	22.5	1988 Sep	1	0.55
IC 5267	Sa	−20.4	1695	22.4	1986 Oct	2	0.47

© American Astronomical Society • Provided by the NASA Astrophysics Data System

1991ApJ...370..526C

2–3 hr was spent this way on each field. Time permitted two fields to be observed for four of the galaxies. The fraction of the whole galaxy observed ranged from 7% for NGC 1291 (by far the closest) to 66% for NGC 1302. The coverage factors were estimated by comparing the Fabry-Perot fields with plates of the galaxies. These will be needed to correct the observed H II region luminosity functions in § 3.

Calibration flat-field and arc-lamp exposures were also taken at the telescope, and the usual debiasing and flat-fielding of the CCD frames was performed.

The most satisfying results in this project can actually be seen in the raw data. We now briefly discuss the observations of each of the galaxies in this program.

Figure 1 (Plate 24) is a montage of three images. The top two are raw Fabry-Perot images of the eastern field of the Sombrero: the left-hand one is off Hα, and the right-hand one is on-band. About 15 emission regions can be seen in the on-band frame. The lower portion of the figure is a composite of all the on-band data, and thus reveals all the detected H II regions, some 50 in number. Comparison with a *B* CCD frame (Fig. 8) indicates a good correspondence with the knots in the disk that were the subject of the debate between Schweizer (1978) and van den Bergh (1976). One of the H II regions found by Schweizer is seen at $X = 230$ and $Y = 65$ in this figure. Given the aspect of this galaxy, it is difficult to say where the H II regions lie in the plane with any precision, but they do appear to lie at about the same radius. About 60 distinct regions were identified in the two fields observed.

Figure 2*a* (Plate 25) shows a similar off-band/on-band montage for one of the two fields of NGC 1371; here more than 100 regions are seen, with 344 regions cataloged in both fields. One region clearly shows a shell structure. Figure 2*b* (Plate 26) is a montage of one the fields observed in IC 5267. The H II regions in that galaxy show a feature also seen in NGC 1302 and NGC 1079: broadly distributed regions at large radii, and an inner arm with closely spaced H II regions.

The on-band Fabry-Perot frames for the six other galaxies are shown in Figures 3*a*–3*c* (Plates 27–29). Only the east ernmost of the two fields observed for NGC 1302 is shown. Except for NGC 1291 and NGC 1398, all of these galaxies are shown in *B* CCD frames in Figure 8, with the Fabry-Perot fields being approximately centered on the center of the broad-band frames (the two frames for NGC 1079 do not correspond so well). The field observed for NGC 1398 was centered on its western arm, while that for NGC 1291 was centered 4.'5 northwest of the nucleus. We note in passing that no nuclear star formation sites were detected in the Sa galaxies for which we observed the nucleus (all except NGC 1291 and NGC 1371).

2.3. Hα *Luminosities*

Having discovered about 1000 H II regions in seven Sa galaxies, we now describe the more detailed reduction and analysis of the Hα data.

The reduction of the Fabry-Perot data is exceptional, in the sense that we did not make a data cube for each field as is the usual practice (cf. Schommer et al 1988). Since we are interested in creating spectra of entire H II regions as opposed to spectra of spatial resolution elements, we elected to extract aperture data at preselected locations from each of the Fabry-Perot frames for each galaxy.

The raw Fabry-Perot images have a 9% reflection off of the CCD surface about the optical axis (see Figure 3*b*, NGC 7410, for an example of a reflected star). Luckily, this can easily be dealt with in software, by rotating the image 180° and subtracting 9% of the rotated image from the original frame. These corrected frames were used only in the process of identifying the H II regions. The corrected frames were inspected on an image display, and coordinates for suspected regions were recorded in a file. The velocity field of the galaxy as well as the radial wavelength falloff of the images meant that not all of the regions were brightest on the same frames. After one frame was inspected, the H II regions identified there were marked on the next frame to be worked on. This routine was repeated to the last frame, whereupon the entire list of coordinates was marked on each frame, and every frame was reinspected so that any missed regions could be easily spotted. The aperture centers were estimated by eye only (to within a few tenths of a pixel), since an automatic centering code would fail to work on many of the more diffuse regions.

Kennicutt, Edgar, & Hodge (1989, hereafter KEH) recently published a detailed photometric study of the H II region populations in late-type galaxies (Sb–Irr), and, in order to make our results as directly comparable to theirs as possible, we adopted a similar operational definition of a single H II region and used a similar measuring technique. Blends were separated into distinct regions if more than one intensity maximum existed with minima in between. In many cases these regions were too close to measure separately, and so the whole complex was measured and a weighting factor applied afterward. This step was essential for the Sc galaxy, which had very few well-separated regions. Aperture sizes for the regions were estimated visually, and were usually limited by confusion, that is, the apertures were chosen so as not to run into too many other apertures. Where many apertures were close together, all were encompassed in a large aperture, whose flux was then divided up using the smaller aperture's fluxes as weights. The aperture diameters tended to lie within the range of 4–8 pixels (270–540 pc at a distance of 20 Mpc); some complexes were measured with apertures of 12–16 pixels (820–1080 pc). The seeing ranged from 2 to 3 pixels FWHM; thus the diameters of H II regions with sizes of 100–200 pc (common in nearby galaxies) will be unresolved, although the emission will still be easily detected.

Before extracting the apertures, the sky region in each frame was inspected for night-sky emission lines, which would of course appear as rings. Where present, these skyline rings could affect the aperture measurements severely, and thus were removed from the frames by finding the radial intensity variation (from the center of the image) in regions free of H II regions and then subtracting that variation from the entire frame. The mean value for the sky region in such frames would then be zero. For data that had no sky rings, the sky continuum level was measured in a region free of H II regions or other galaxy light. In contrast to the procedure in KEH, we do not subtract off a local background, determined in an annulus around the aperture. Since we have actual spectra, the continuum is the local background. We merely have to subtract off the flux from the sky in the aperture, the sky having the same intensity level for the whole data frame.

Intensities were then extracted for the apertures from each frame (via a simple digital aperture program) and stored in a file. We then subtracted off the sky contribution and corrected the intensity for each aperture to zero air mass, and finally calculated the wavelength for the particular location of that aperture in the frame. Thus a list of intensity-wavelength pairs for each identified H II region was created.

© American Astronomical Society • Provided by the NASA Astrophysics Data System

1991ApJ...370..526C

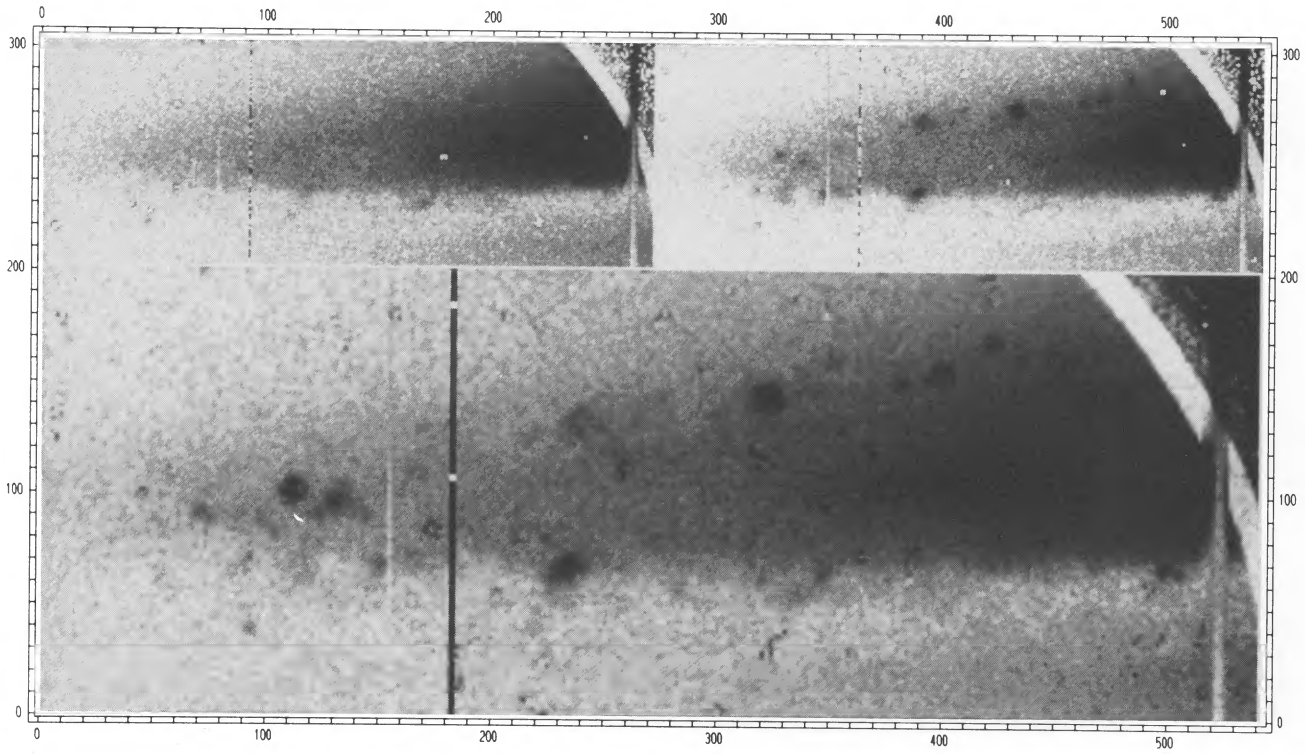

FIG. 1.—Fabry-Perot images of NGC 4594 (the Sombrero). The top left-hand frame is part of a raw image, taken off the redshifted wavelength of Hα. At the top right is an on-band picture, showing some of the H II regions in this galaxy. All of the detected H II regions for this field can be seen in the bottom panel, which is a combination of several on-band images.

CALDWELL et al. (see 370, 528)

© American Astronomical Society • Provided by the NASA Astrophysics Data System

1991ApJ...370..526C

PLATE 25

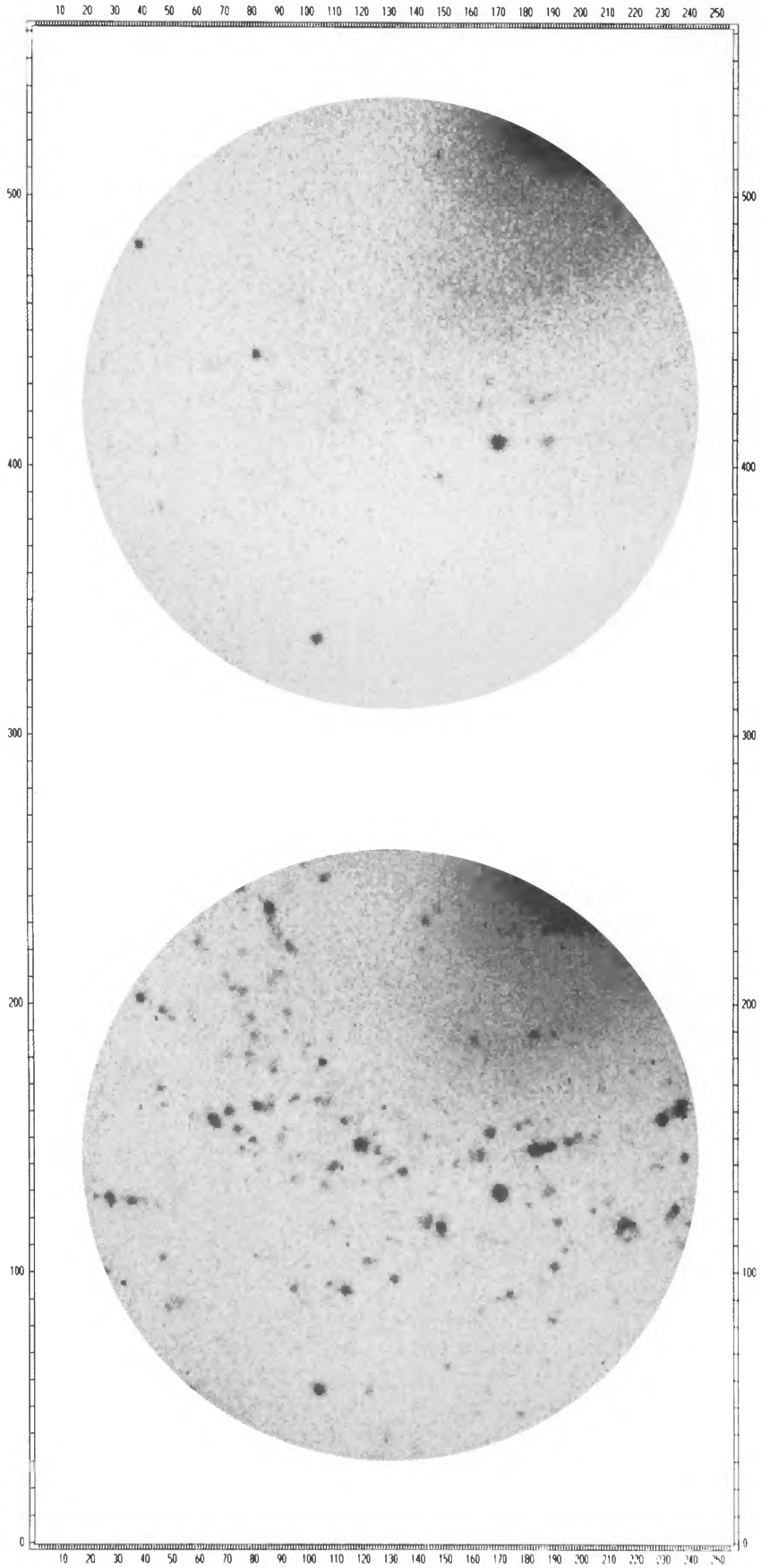

FIG. 2a

FIG. 2.—(*a*) A pair of frames for NGC 1371, one off Hα and one on Hα. The on-band frame is a combination of all the on-band frames, as are all the rest of the on-band frames to follow. (*b*) A similar pair of frames for IC 5267.

© American Astronomical Society • Provided by the NASA Astrophysics Data System

1991ApJ...370..526C

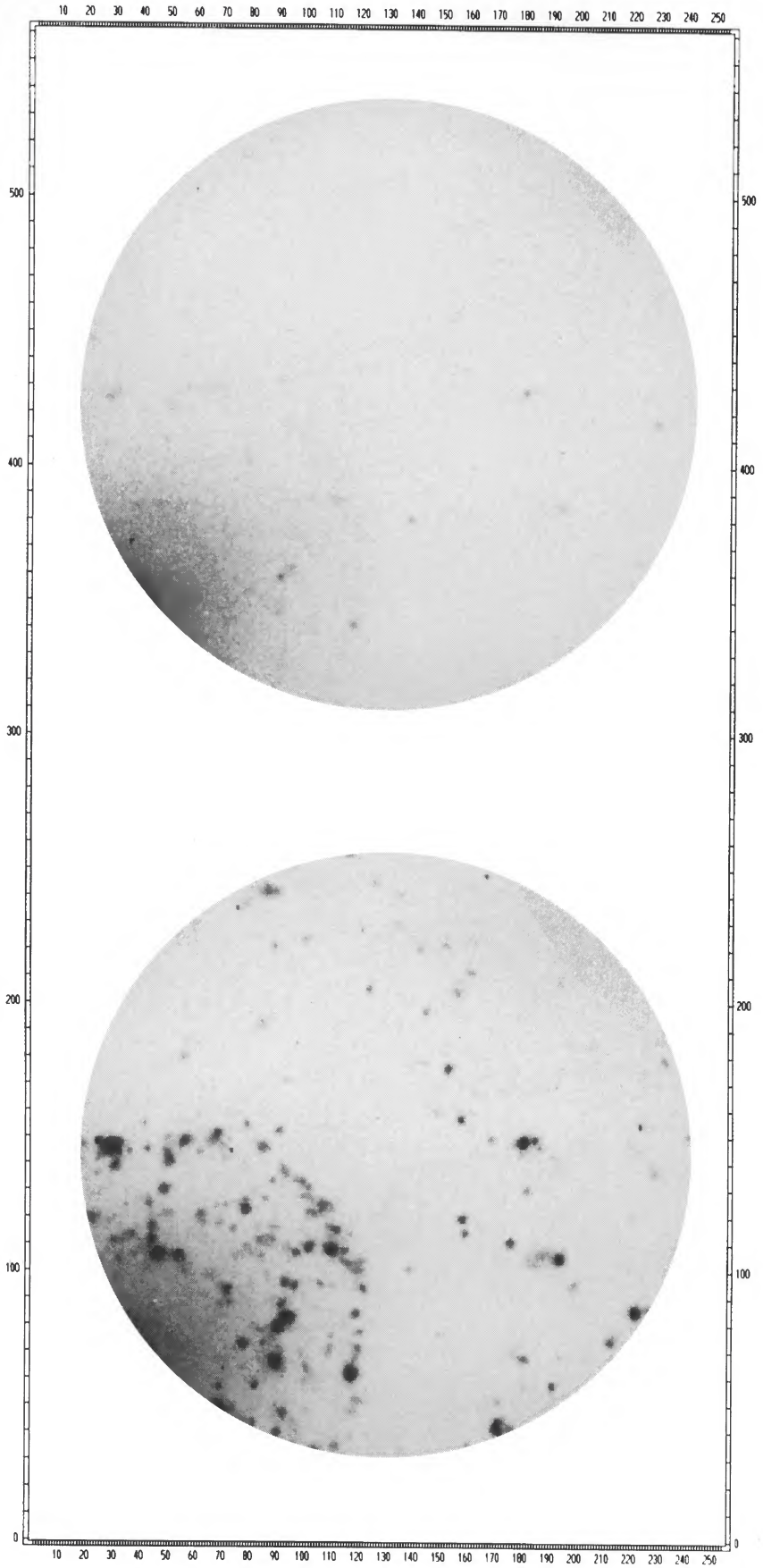

FIG. 2*b*

CALDWELL et al. (see 370, 528)

© American Astronomical Society • Provided by the NASA Astrophysics Data System

1991ApJ...370..526C

PLATE 27

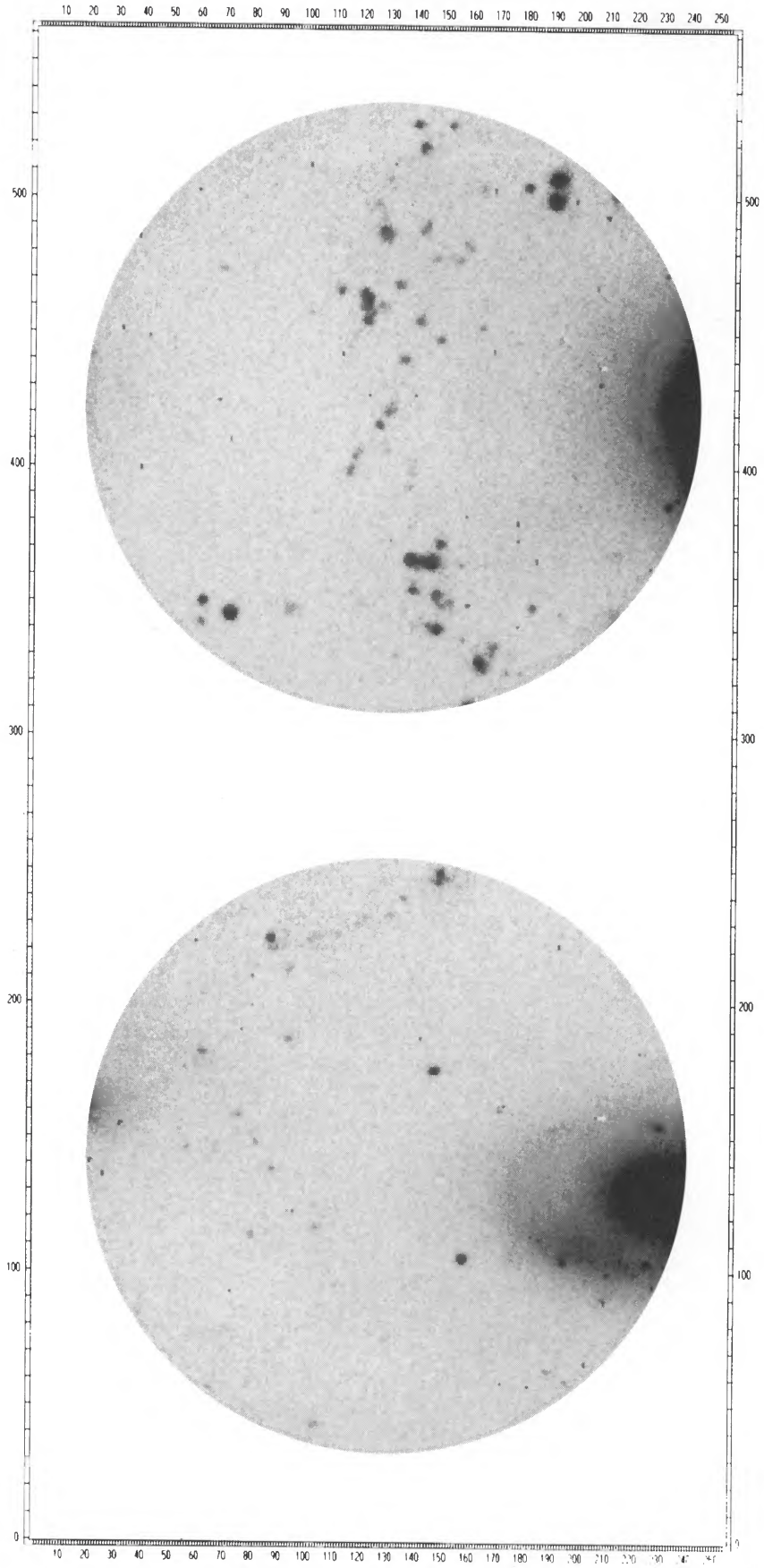

FIG. 3a

FIG. 3.—(*a*) On-band frames for NGC 1302 and NGC 1079. (*b*) NGC 7410 and NGC 1291. (*c*) NGC 1398 and NGC 7689.

© American Astronomical Society • Provided by the NASA Astrophysics Data System

1991ApJ...370..526C

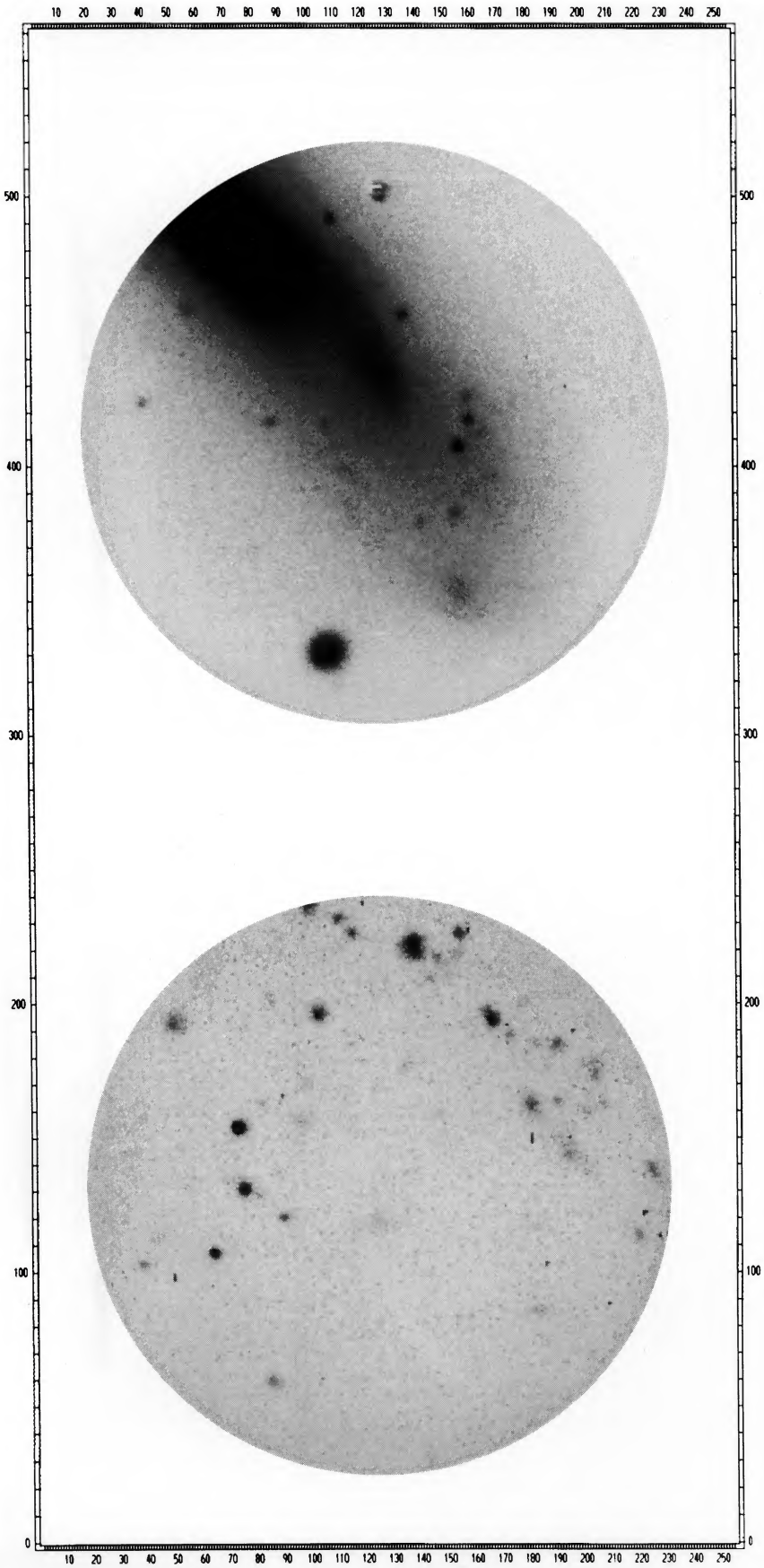

FIG. 3*b*

CALDWELL et al. (see 370, 528)

© American Astronomical Society • Provided by the NASA Astrophysics Data System

1991ApJ...370..526C

PLATE 29

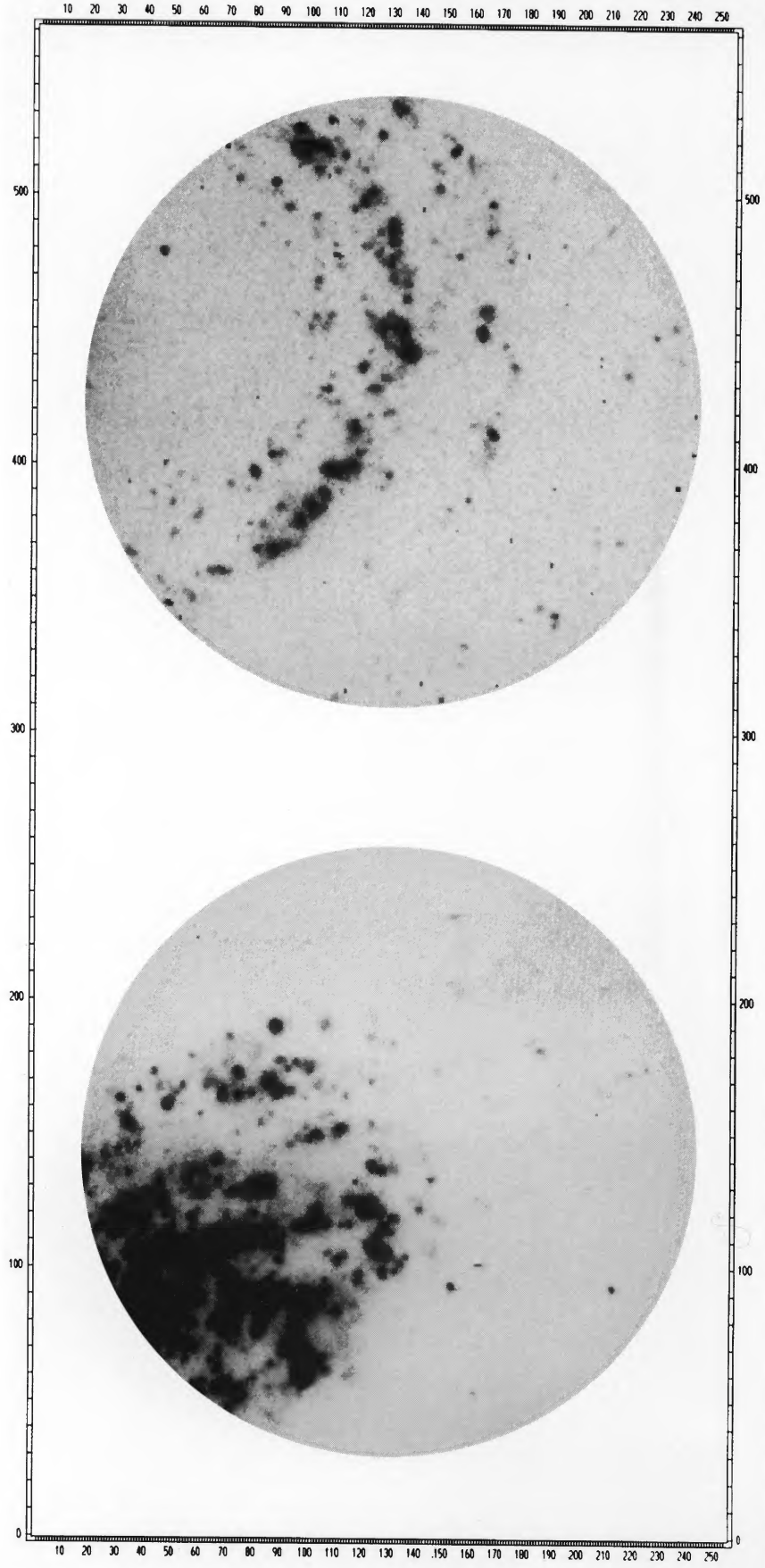

CALDWELL et al. (see 370, 528)

© American Astronomical Society • Provided by the NASA Astrophysics Data System

1991ApJ...370..526C

From these *spectra* we can extract Hα luminosities and velocities by fitting Gaussian functions to the data. We chose not to measure the velocity dispersions because the 2.4 Å resolution of the etalon corresponds to a velocity dispersion of 47 km s^{-1}, much greater than we expect to see for most H II regions. For the least-squares fits we fixed the dispersion at 47 km s^{-1} and solved for the velocity, continuum, and intensity amplitude. Combining those quantities with a galaxy's distance, we derived a luminosity in Hα. The luminosity is not greatly affected by the decision to fix the velocity dispersion, because differences between the true dispersion and the assumed value are partly taken up in the amplitude value of the Gaussian, thus leaving the integral of the Gaussian unchanged to first order. The zero point for the fluxes was set by observations of a few spectrophotometric standard stars, observed each night (all of the nights were photometric).

For a distance of 20 Mpc, the luminosity of an H II region with a positive detection was about $10^{36.6}$ ergs s^{-1}. Few real H II regions with luminosities less than $10^{36.2}$ ergs s^{-1} were detected. We attribute most of the paucity in low-luminosity H II regions to identification problems and blending. The great power of the Fabry-Perot instrument is apparent when one realizes that the KEH data for the Large Magellanic Cloud and M101 extend only to $L(\mathrm{H}\alpha) = 10^{36.8}$ ergs s^{-1} for these nearby galaxies.

Schweizer (1978) gave a luminosity for one of the H II regions in the Sombrero that he found. Changing his value to accommodate our assumed distance, we find our luminosity for that region to be 4 times higher than his, which, it happens, is the error Schweizer attached to his measurement. This particular H II region is actually twice as large in diameter as he assumed for his calculation. As a check on the physical conditions in the emission regions discovered in the Sombrero, we also took Fabry-Perot frames centered around the redshifted [N II] 6583 Å line for both of the Sombrero fields imaged. As expected for H II regions, the Hα/[N II] ratio was greater than 3 for the cases in which the detection of [N II] emission was significant.

3. H II REGION LUMINOSITY FUNCTIONS

While we have made the important observation that H II regions are common and abundant, the quantitative aspects of the star formation in Sa's can be studied best by examining the Hα luminosity functions (LFs), and comparing them with those already measured for the later type galaxies. In this section we will create such luminosity functions, but first we review what is known about the LFs in later type spirals, work done by KEH and Kennicutt (1988). Bright H II regions have a luminosity function that is well represented by a power law:

$$N = AL^a \delta L ,$$

where A is a normalization constant. The Im galaxies brighter than $M_V = -17$ have shallow H II region luminosity functions and some of the largest complexes known (e.g., 30 Doradus in the LMC). The Sbc–Sc galaxies have somewhat steeper LFs (slope $a = -2$ as opposed to -1.7 for the Im types) and fewer regions per unit stellar luminosity (mostly because the Im's are smaller galaxies). The Sab and Sb galaxies have fewer H II regions still, and none with $L(\mathrm{H}\alpha) > 10^{39}$.

Table 2 presents a summary of the Hα measurements made here. The total number of H II regions listed in column (2), followed by the raw total Hα luminosity from H II regions in ergs per second, the Hα luminosity corrected for the fraction of the galaxy observed, and the global Hα luminosity (see below, § 5).

In calculating the LFs for the galaxies in this program, we have excluded regions with uncertain detections (effectively eliminating all H II regions with luminosities less than $10^{36.6}$ ergs s^{-1}), and have applied a multiplicative correction to the samples to account for the fraction of the whole galaxy observed. The data were binned into 0.2 dex intervals.

The LFs for some late-type galaxies from previous photographic and CCD work (KEH) are presented in Figure 4. The LMC LF extends to high-luminosity regions, and has a shallow slope, meaning that there are relatively many regions at high L as compared with low L. M31 and NGC 2841, both Sb galaxies, have few high-L regions, and have a steeper slope: fewer bright regions per faint regions. Figures 5*a*–5*c* show the individual LFs for all of the galaxies in this study. The dashed line represents the actual measurements, while the solid line contains the correction factor. None of these Sa's have H II regions with luminosities greater than $10^{38.4}$ ergs s^{-1}, while at the other end, regions as faint as the detection limit ($10^{36.0}$ ergs s^{-1}) are present in small numbers. There is clearly also a large dispersion in the properties of the Sa galaxies: IC 5267 and NGC 1371 have hundreds of star formation sites, while NGC 7410 and NGC 1079 are rather poor in that regard. Indeed, the former two galaxies are both more abundant than NGC 2841 in H II regions fainter than $10^{38.4}$ ergs s^{-1}, and IC 5267 is more abundant than M31 at such luminosities. We are approaching the time when it will become more sensible to rank galaxies by their physical properties, one being current star formation rate, rather than by a subjective classification scheme.

TABLE 2

Hα MEASUREMENTS

Galaxy	Number of H II Regions	Logarithm of Measured Hα in Discrete Regions	Logarithm of Corrected Hα in Discrete Regions	Logarithm of Total Hα
NGC 1079	66	39.1	39.6	40.3
NGC 1291	51	38.4	39.6	...
NGC 1302	167	39.7	39.8	39.8
NGC 1371	344	39.6	40.1	40.5
NGC 1398	201	39.7	40.5	40.7
NGC 4594	64	39.2	39.4	...
NGC 7410	42	39.3	39.5	39.3
NGC 7689	301	40.7	41.0	41.1
IC 5267	320	39.9	40.2	40.4

© American Astronomical Society • Provided by the NASA Astrophysics Data System

1991ApJ...370..526C

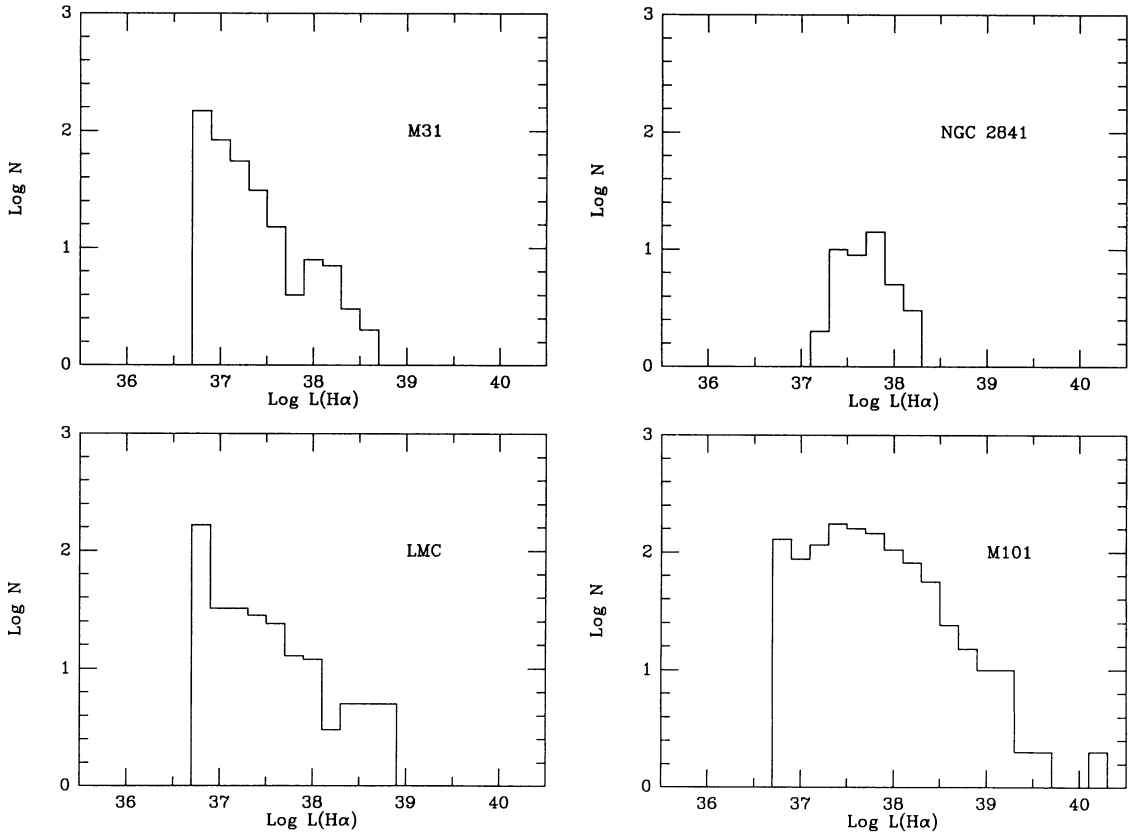

FIG. 4.—Hα luminosity functions for well-known late-type galaxies. The logarithm of the number of H II regions is plotted against the logarithm of the Hα luminosity in ergs s^{-1}. The bin size is 0.2 in the log.

A representative LF was made by combining the individual LFs for NGC 1079, NGC 1302, NGC 1371, NGC 7410, and IC 5267 (NGC 1291 was left out because the galaxy was not well sampled, as can be told from its LF; NGC 4594 was left out because of its high inclination). The numbers were scaled to what would correspond to a single galaxy. Over the region where the data are complete (basically all of the regions brighter than the turnover luminosity), a power law seems as good a fit for the Sa LF as it is for the later types. The slope of the combined LF for Sa's is -2.6, steeper than the value of -2.3 found for the Sab NGC 1398, and much steeper than that for the Sc NGC 7689 which has $a = -2.0$, similar to other Sc's measured photographically.

For most of the late-type galaxies in the KEH study, including those illustrated in Figure 4, the turnover in the LF at low luminosities is due to a combination of incompleteness and crowding effects. Both of these effects are reduced in our sample of Sa galaxies, because the images are deeper and because the lower number density of H II regions reduces the crowding problem. Consequently, the lower luminosity turnovers for the Sa's in comparison to the later-type galaxies is probably purely instrumental. Most of the Sa's have turnovers at around 10^{37} ergs s^{-1}; however, NGC 7410 and NGC 4594 have brighter turnovers. Since these are the two most inclined galaxies in the sample, we suggest that the difference in turnover luminosities is again simply a completeness problem.

The extinction-corrected Lyman continuum luminosities corresponding to the range of Hα luminosities of 10^{37}–10^{39} ergs s^{-1} is of order 10^{49}–10^{51} photons s^{-1}, thus putting these H II regions in between the realm where a star cluster provides the ionization and where a single very massive star could be the source. Thus, other than the obvious result that the presence of Hα requires stars with masses greater than 10 $M_\odot$, we would find it difficult to say whether or not the Sa IMF differs in detail from that found in our own Galaxy. It may be important to note that Hunter & Massey (1990) have collected new data on *Galactic* H II regions with Hα luminosities similar to those in Sa's and find both that the mass function for these low-luminosity star formation sites is no different from that for larger Galactic sites and also that stars as early as O6 V exist in H II regions as faint as $10^{36.9}$ ergs s^{-1}.

To continue the discussion in KEH on the change in LF with Hubble type, we have added up the numbers of H II regions with luminosity above $10^{37.7}$ ergs s^{-1} per unit galaxy luminosity of 10^{10} $L_\odot$ for each of the galaxies observed here. Figure 6*a* shows the progression of this quantity now for the whole range of star-forming galaxies. The Sm–Im galaxies have more than 100 H II regions per unit galaxy luminosity, while the Sa galaxies on average have fewer than 10. If the contribution of the bulge to the total light in the Sa's is removed (see below § 5), the average Sa still has a value of only 12 for this quantity.

The surface densities of H II regions with luminosities greater than $10^{37.7}$ ergs s^{-1} are typically smaller than 0.03 regions kpc^{-2} in an Sa galaxy, a density 30 times less than is found in late-type galaxies (Fig. 6*b*). We concur with KEH that the differences between star formation sites in early-type and late-type spirals are twofold: there are fewer sites at all lumi-

© American Astronomical Society • Provided by the NASA Astrophysics Data System

1991ApJ...370..526C

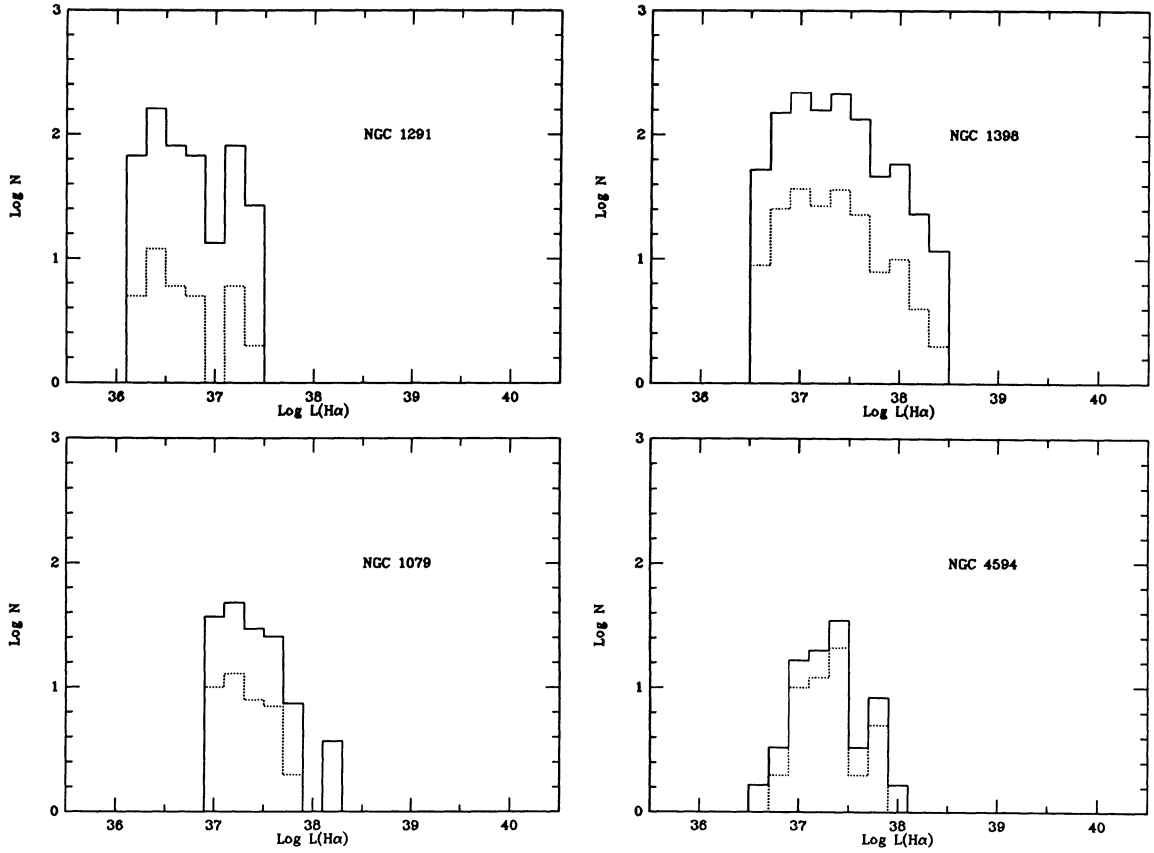

FIG. 5*a*

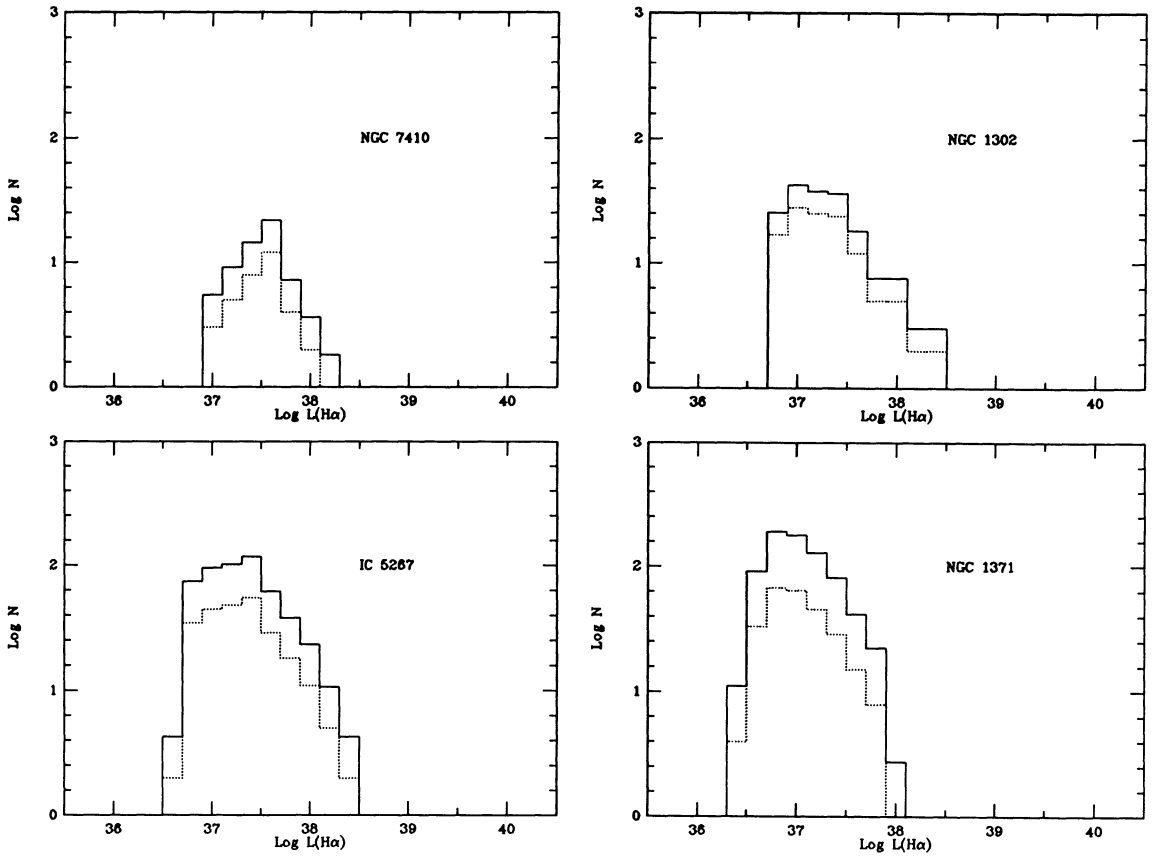

FIG. 5*b*

FIG. 5.—(*a*–*c*) Hα luminosity functions from Fabry-Perot data for galaxies in this study

© American Astronomical Society • Provided by the NASA Astrophysics Data System

1991ApJ...370..526C

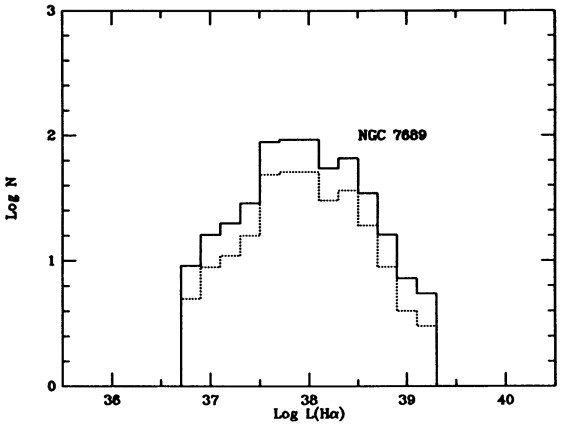

FIG. 5c

nosities for early types, and the largest sites in early types are much smaller than those for late-type galaxies.

4. STAR CLUSTERS

4.1. *Observations and Reductions*

UBV frames are needed for these galaxies for several reasons. First, the question of IMF variation posed earlier in effect asks whether there are any young star clusters that have no massive stars. To answer that in full, we need to know whether many of the blue knots in Sa's have no corresponding H II regions, requiring the colors of the knots to be measured. Second, an inspection of the star cluster LFs for Sa's will alert us to any differences with the already studied star clusters in later type galaxies, differences that might be attributable to differences in the physics of star formation. Third, continuum measurements of the H II regions provide a rough way of calculating the IMF itself. Last, average disk star formation rates can be calculated from the integrated disk light (§ 5). Time did not permit all of the galaxies observed in Hα to be imaged in *UBV*, but the results of those observed should be applicable to those unobserved. Table 3 lists the available *UBV* frames for the galaxies in this study. Full *UBV* data exist only for fields in NGC 1079, NGC 1302, and NGC 1371, while *BV* data are available for IC 5267 and one of the NGC 1302 fields. Frames were taken of NGC 4594, but they proved to be useless for the quantitative measurements in this study, again because of the high inclination of that galaxy. Fairly good overlap was obtained between the Fabry-Perot images and the *UBV* data for all of the galaxies except NGC 1079, in which case about half of the H II regions found on the Fabry-Perot images fell outside of the area observed in broad band.

TABLE 3

UBV DATA

Galaxy	Number of Fields	Filters
NGC 1079	1	*UBV*
NGC 1302	1	*UBV*
NGC 1302	1	*BV*
NGC 1371	2	*UBV*
NGC 4594	1	*UBV*
IC 5267	1	*BV*
NGC 7689	1	*UBV*

The CTIO 4 m PFCCD system was used for most of these observations. At the time, the system employed on RCA CCD, giving a pixel scale of 0".6 pixel^{-1}. Standard stars taken during the night were used to calibrate the *UBV* frames onto the system defined by Graham (1981). Transformations to standard magnitudes and colors should be accurate to about 1% in the *B*-magnitudes, 4% in $B-V$, and 5% in $U-B$. An exception is the data for IC 5267, for which no contemporaneous standard stars were observed. The data can still be calibrated with integrated aperture photometry of the entire galaxy, provided in Bucknell & Peach (1976). Exposures of the galaxies were typically 15 minutes in *B* and *V*, and 1000 s in *U*. The seeing ranged from 1".4 to 2".3 FWHM. Several of these are shown in Figures 7*a*–7*b* (Plates 30 and 31). NGC 1371 in particular shows very good resolution into what appear to be clusters. The Sc galaxy NGC 7689 was observed with the 1.5 m telescope at CTIO, and the data were treated in a similar manner to the 4 m data.

To provide the numbers needed for the comparisons described above, aperture photometry was extracted from the *UBV* frames, using digital photometry techniques similar to those used in Caldwell & Phillips (1989). Knots were visually identified on frames that had been processed to remove the low-frequency component due to the galaxy's overall light distribution. The instrumental photometry was extracted for those knots using an aperture 1 FWHM in diameter and transformed to standard *B*-magnitudes and *UBV* colors using the transformations provided by standard stars. The apertures used for these knots did not contain all of the light, for two reasons: (1) the actual point-spread functions have a limiting radius larger than the apertures used, and (2) the knots are occasionally resolved. We applied an aperture correction determined from stars on the same field to account for the first, but choose to ignore the second, since many of the knots are blended anyway.

The next step in our analysis is the cross-referencing of the Hα measurements with the broad band. This was accomplished by using the stars to be found in the fields to provide coordinate transformations. An acceptable identification was one in which the center of the *B* aperture fell somewhere within the H II region aperture. This seems reasonable, since in many known H II regions the peak in emission-line intensity is not the same location as the peak in continuum intensity. H II region apertures which lay off the broad-band field were noted also, as well as the reverse.

4.2. *Correlation of Colors and* Hα *Luminosities*

For NGC 1079, 54 knots that lay on the Fabry-Perot fields were measured on the broad-band CCD frames, 22 of which had been also identified as H II regions. For NGC 1302, 104 knots were measured, 60 of which have Hα. For NGC 1371, the numbers are 111 and 81, and finally, for IC 5267, 91 knots were measured, 51 of which have Hα. The occasional presence of Hα without an associated continuum knot speaks of the possibility of finding discrete Hα in even earlier galaxies like S0a's or even S0's that have no obvious continuum knots.

A remaining qualitative question is the frequency of the occurrence of blue knots without accompanying emission from ionized gas. If the mass function were depleted in stars with $M > 10\ M_\odot$ everywhere, then we would not see any Hα anywhere. The data have already ruled that possibility out, and so a weaker postulate to test might be to assume that the presence of a large number of blue star clusters without Hα means the

© American Astronomical Society • Provided by the NASA Astrophysics Data System

1991ApJ...370..526C

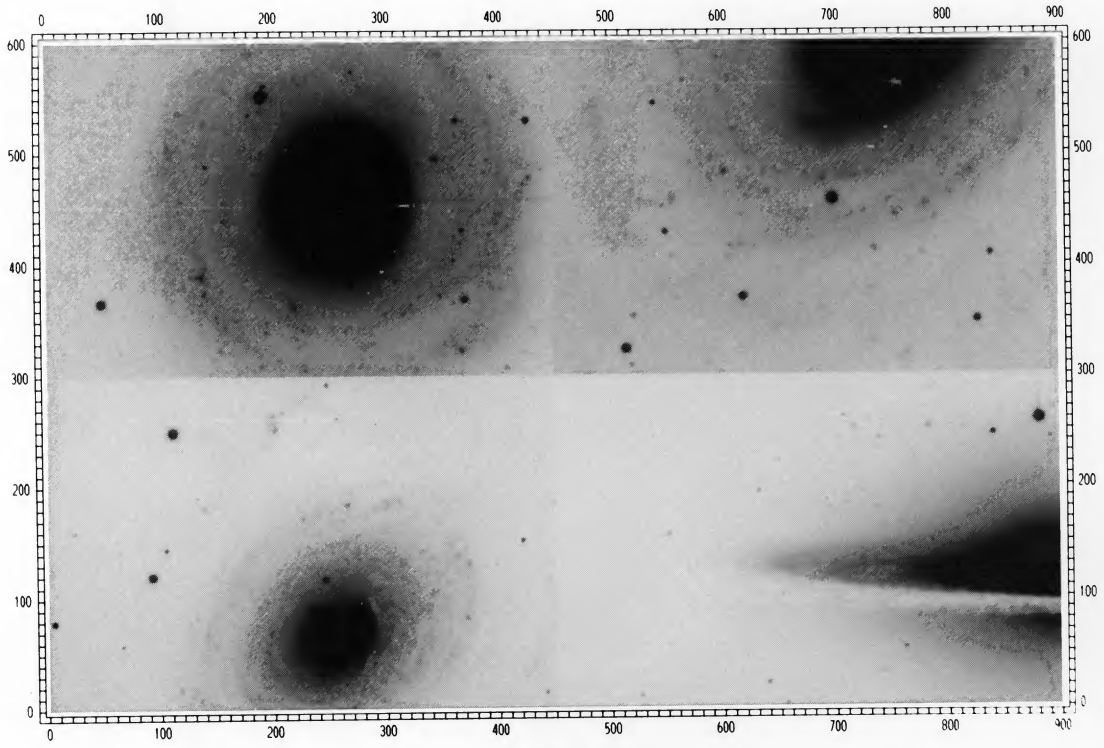

FIG. 7a

FIG. 7.—(*a*) *B* CCD images of NGC 1302, NGC 1371, IC 5267, and NGC 4594. (*b*) *B* CCD images of NGC 1079, NGC 7410, and NGC 7689 (an Sc).

CALDWELL et al. (see 370, 532)

© American Astronomical Society • Provided by the NASA Astrophysics Data System

1991ApJ...370..526C

PLATE 31

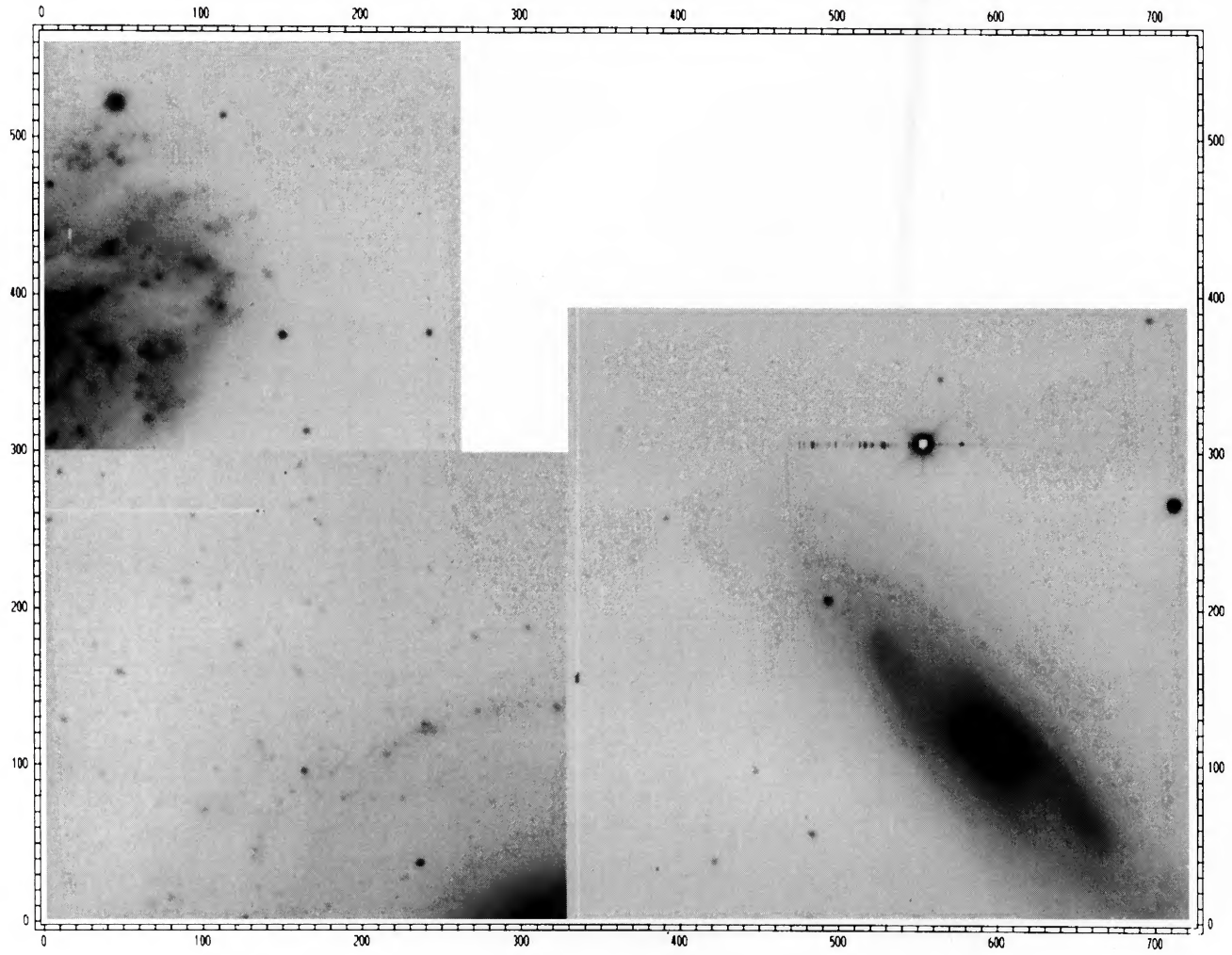

CALDWELL et al. (see 370, 532)

© American Astronomical Society • Provided by the NASA Astrophysics Data System

1991ApJ...370..526C

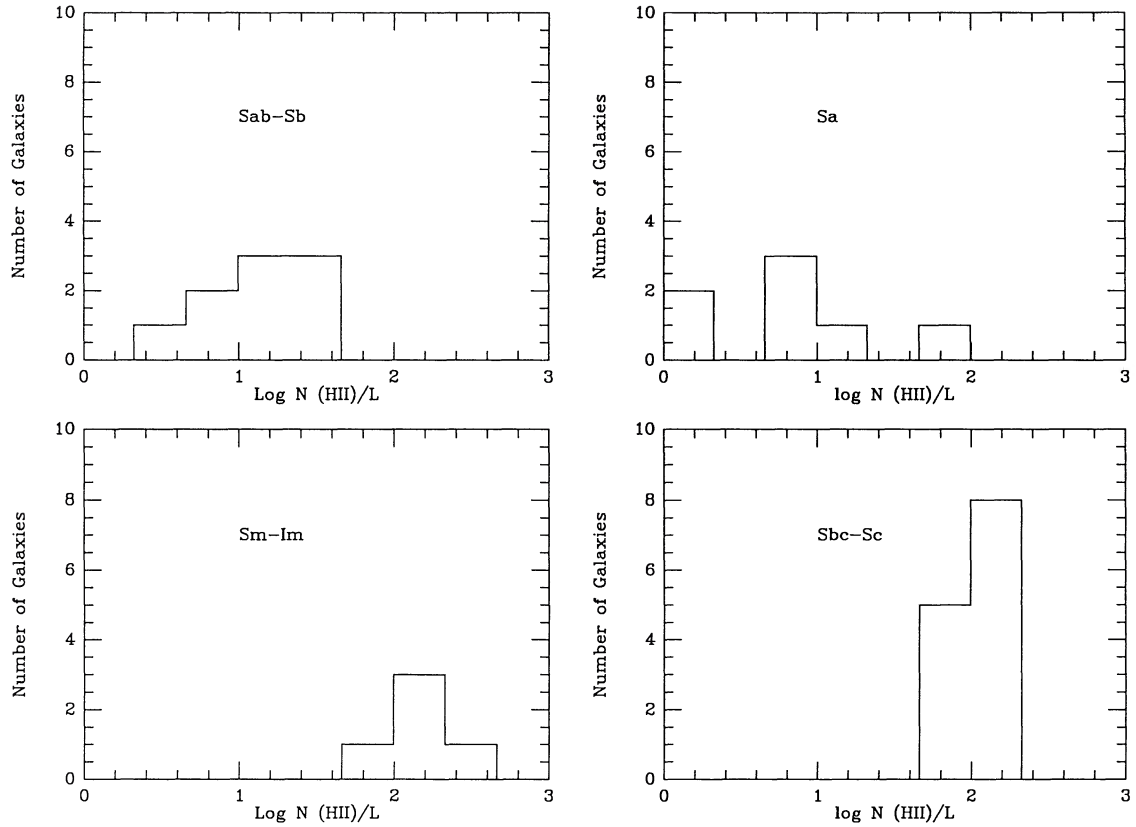

FIG. 6*a*

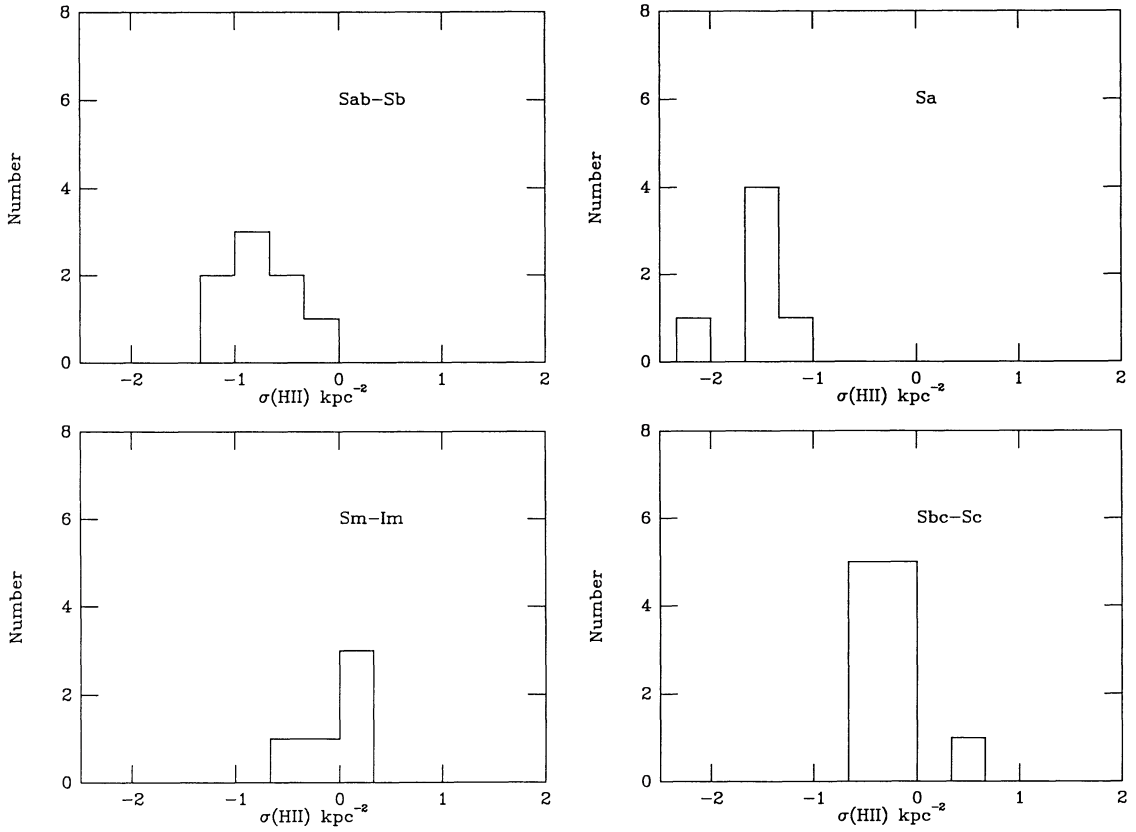

FIG. 6*b*

FIG. 6.—(*a*) Progression of bright H II region content as a function of Hubble type. Shown are histograms of the number of galaxies studied as a function of the number of H II regions they contain with Hα luminosities log L(Hα) > 37.7, normalized in galaxy luminosity. Data for the non-Sa's in (*a*) and in (*b*) are from KEH. (*b*) Progression of the surface density of bright H II region content as a function of Hubble type. Shown are histograms of the number of galaxies studied as a function of the surface density of H II regions they contain with Hα luminosities log L(Hα) > 37.7.

© American Astronomical Society • Provided by the NASA Astrophysics Data System

1991ApJ...370..526C

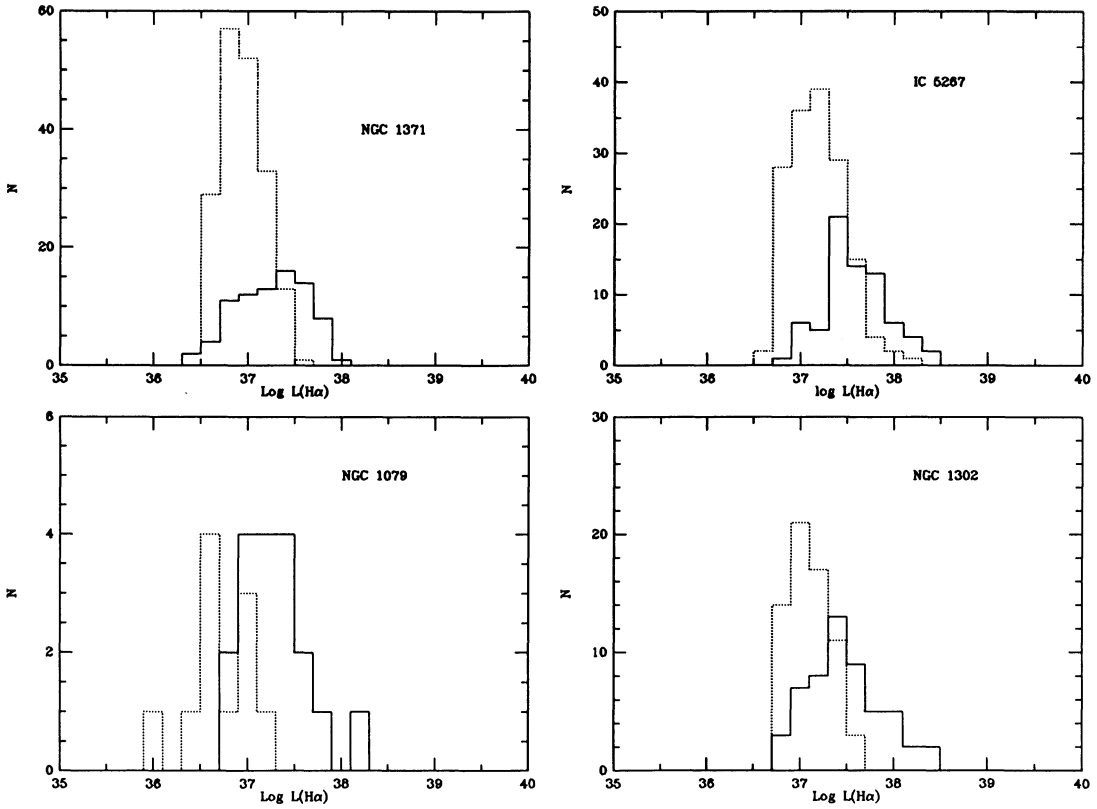

FIG. 8.—Hα luminosity functions broken up into those regions that were detected in the continuum (*continuous lines*) and those that were not (*dotted lines*)

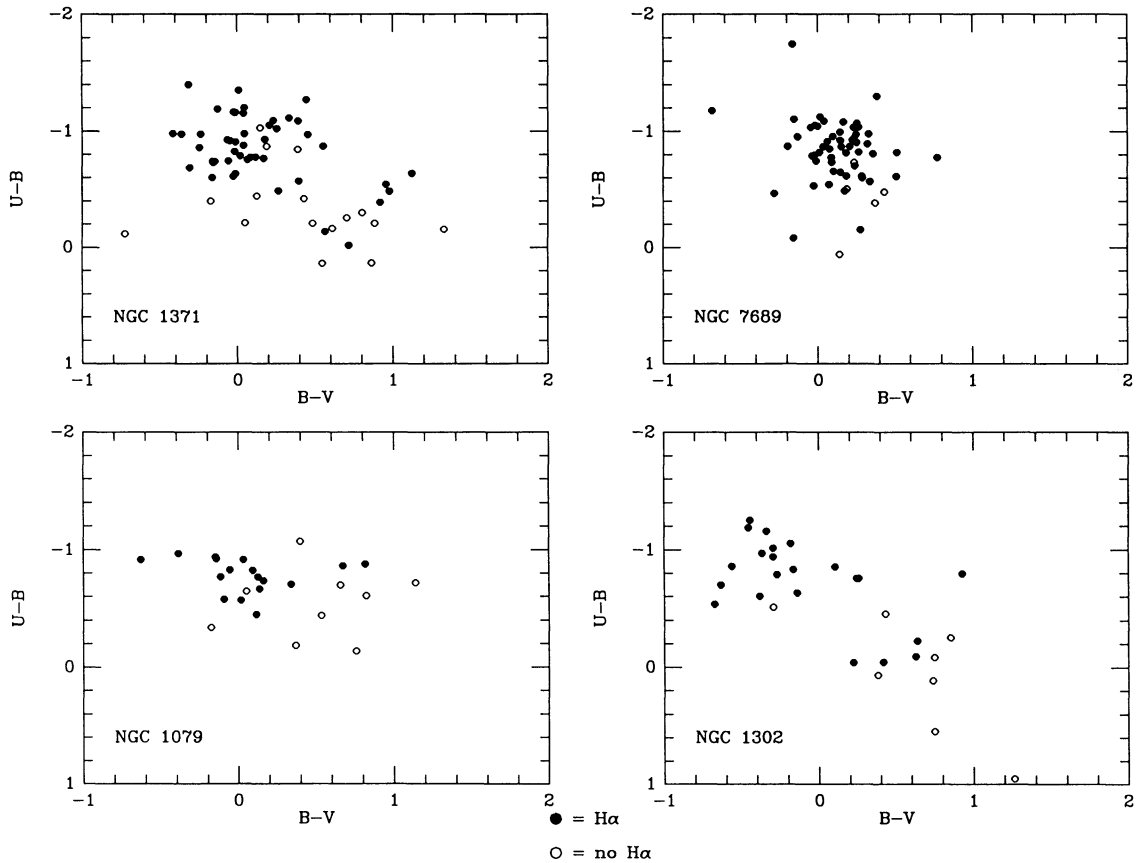

FIG. 9.—Color-color diagrams for the continuum knots. Filled circles show knots detected in Hα, while open circles represent those without Hα detections.

© American Astronomical Society • Provided by the NASA Astrophysics Data System

1991ApJ...370..526C

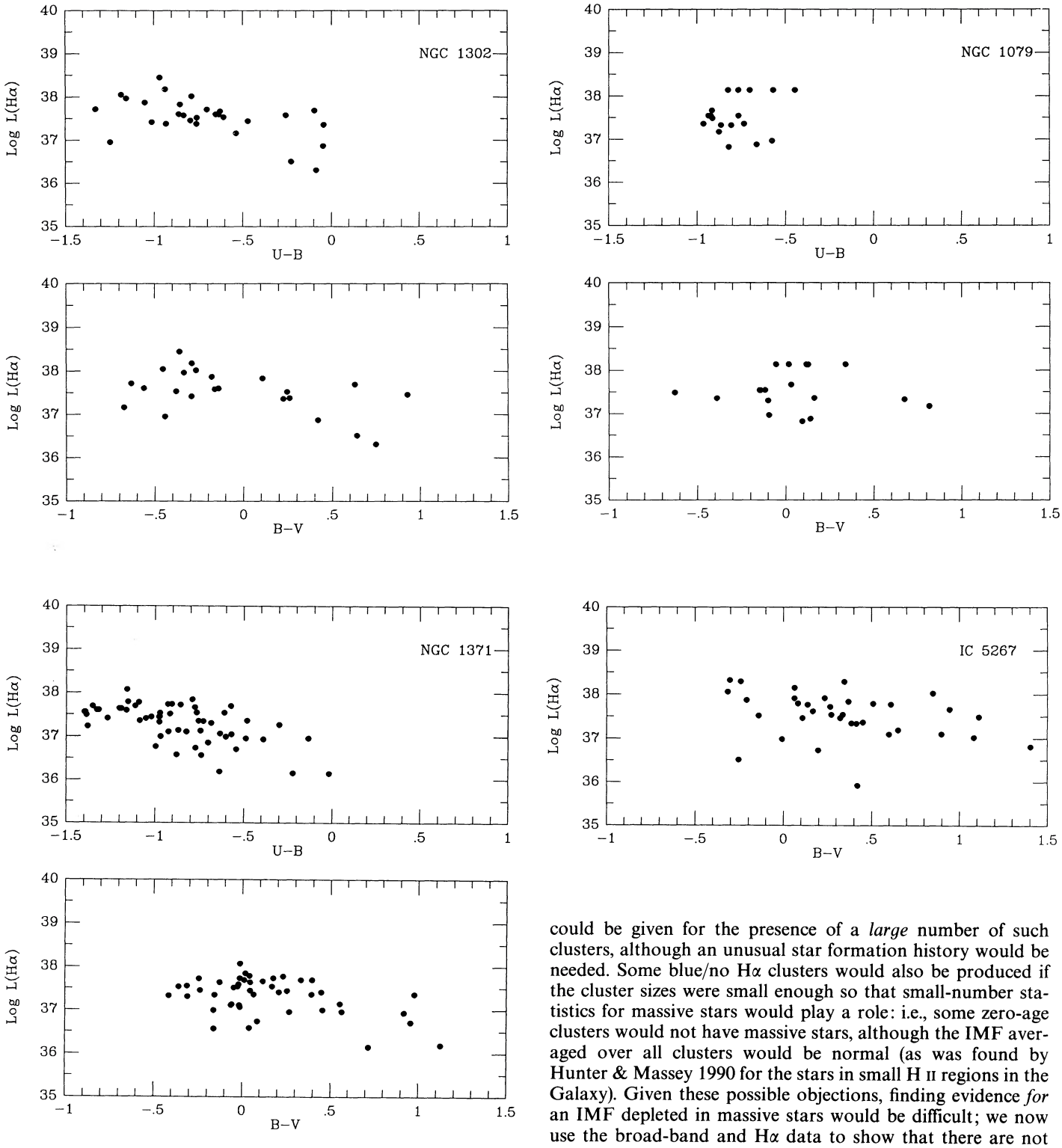

FIG. 10.—Color-Hα luminosity diagrams. The bluer knots tend to be the brightest H II regions as well.

mass function in the galaxy varies from place to place. Since the presence of *some* blue clusters without Hα in late-type galaxies can easily be attributed to age differences in the cluster population (optical colors are insensitive to 10 Myr age differences), we should be concerned that the same reason could be given for the presence of a *large* number of such clusters, although an unusual star formation history would be needed. Some blue/no Hα clusters would also be produced if the cluster sizes were small enough so that small-number statistics for massive stars would play a role: i.e., some zero-age clusters would not have massive stars, although the IMF averaged over all clusters would be normal (as was found by Hunter & Massey 1990 for the stars in small H II regions in the Galaxy). Given these possible objections, finding evidence *for* an IMF depleted in massive stars would be difficult; we now use the broad-band and Hα data to show that there are not many such blue/no Hα regions which would prompt discussion in the first place.

Our analysis will focus on several diagrams (Figs. 8–11) showing colors, magnitudes, and Hα luminosities. Figure 8 shows the raw Hα luminosity functions for the galaxies broken up into those regions that were detected in the continuum (*continuous lines*) and those that were not (*dotted lines*). Most H II regions with luminosities above $10^{37.7}$ ergs s^{-1} were

© American Astronomical Society • Provided by the NASA Astrophysics Data System

1991ApJ...370..526C

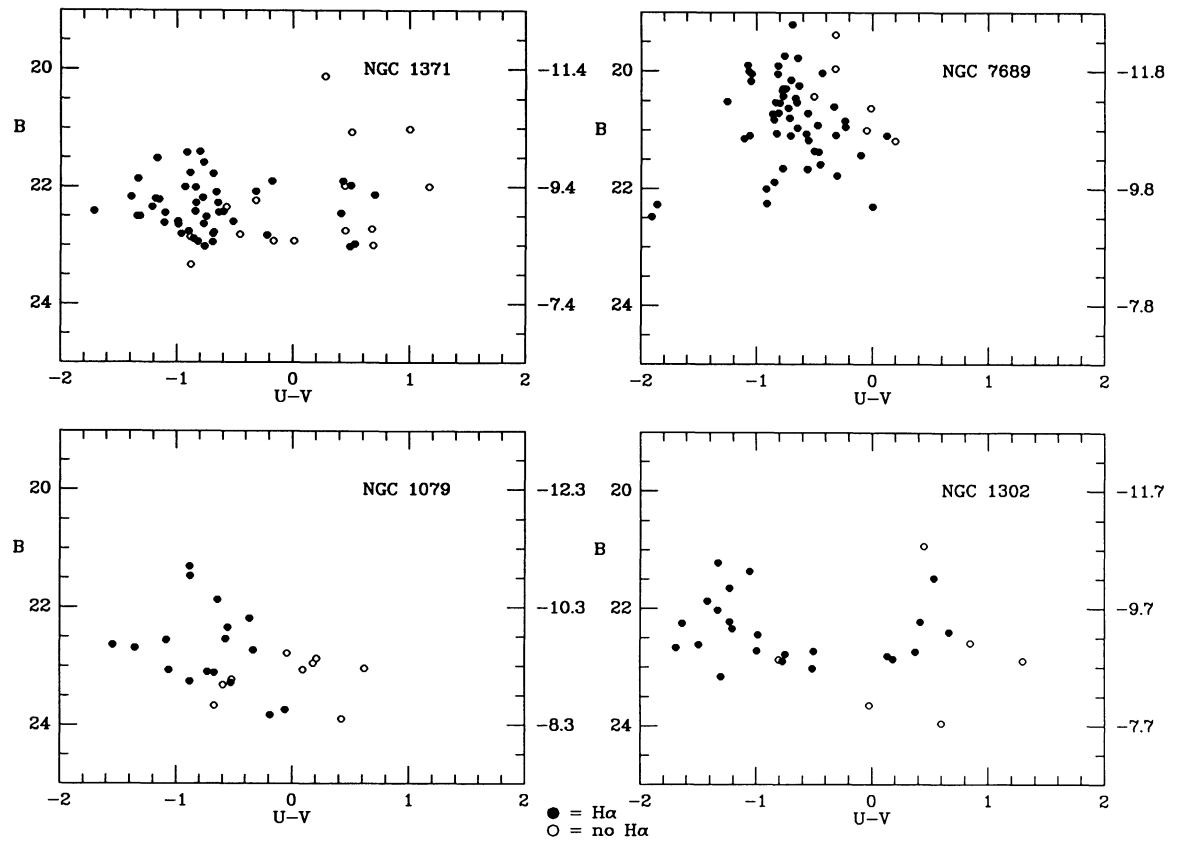

FIG. 11.—Color-magnitude diagrams for the continuum knots. Symbols are as in Fig. 10. The absolute magnitude scale at the right assumes the distances listed in Table 1.

detected in the continuum (meaning that they had B-magnitudes brighter than 24.2, or $M_B = -7.3$). Not too many H II regions with luminosities below $10^{37.0}$ ergs s^{-1} were detected in the continuum. A few bright H II regions in IC 5267 were not seen in continuum; most of these are very diffuse but large regions.

Figure 9 shows for the continuum knots in each galaxy a $U-B$, $B-V$ diagram, with distinguishing symbols for those knots that were detected in Hα and those that were not. Here we see that, as expected, the very bluest knots in both $U-B$ and $B-V$ tend to have associated H II regions. Also shown are the data for the Sc, for which there was essentially a one-to-one correspondence between the H II regions and the continuum knots.

Another expectation is confirmed in Figure 10, which shows that the bluest knots, in both $U-B$ and $B-V$, are the most luminous H II regions as well. Figure 11 shows the color-magnitude diagrams for the fields observed. We see that most of the observed knots (and hence H II regions) have apparent blue magnitudes fainter than 21, and thus absolute magnitudes fainter than −10.5.

4.3. *Continuum Luminosity Functions*

Figure 12 shows the B luminosity functions for all of the knots in the CCD fields. The functions for the four Sa's shown all peak between $-9 < M_B < -8$, whereas the function for the Sc has a brighter peak at $M_B \sim -11$. The slopes appear to be similar, with a power-law exponent of −2 for the Sa's, and −1.5 for the Sc, though the latter is uncertain because of the difficulty of measuring the clusters in the dense field of that galaxy. These distinctions in the B luminosity functions are consistent with what was seen in the Hα LFs earlier, as would be expected if most of the bright star clusters are directly or indirectly associated with the H II complexes. It would be very productive to obtain similar UBV data for a large sample of late-type galaxies, in order to compare the cluster/association properties directly with those in the Sa galaxies discussed here.

If the IMFs in these early-type galaxies are systematically depleted in the most massive stars, as was suggested by van den Bergh (1976), the one would expect the integrated Hα luminosities of the clusters to be much more affected than their blue luminosities. Hence a simple test of the van den Bergh claim is to compare the ratio of the Hα and B fluxes of the brightest H II regions in Sa galaxies with H II regions in late-type spirals. We measured this ratio for the brightest five H II regions in IC 5267, NGC 1079, NGC 1302, and NGC 1371 (20 regions in total) and found a mean value which was virtually the same as for the six brightest H II regions in the Sc NGC 7689, and also for the three brightest H II regions in M 101 (data from Sandage & Tammann 1974 and Kennicutt 1988; the value is 18 in units of 10^{33}). While this does not prove that the upper mass ends of the IMFs in the Sa galaxies are necessarily the same as in Sc galaxies (the luminosities of the respective H II regions are factors of 10–1000 different, and consequently our treatment of the Hα/B ratio as an IMF index is simplistic), it does exclude the extreme IMF differences which were proposed previously.

© American Astronomical Society • Provided by the NASA Astrophysics Data System

1991ApJ...370..526C

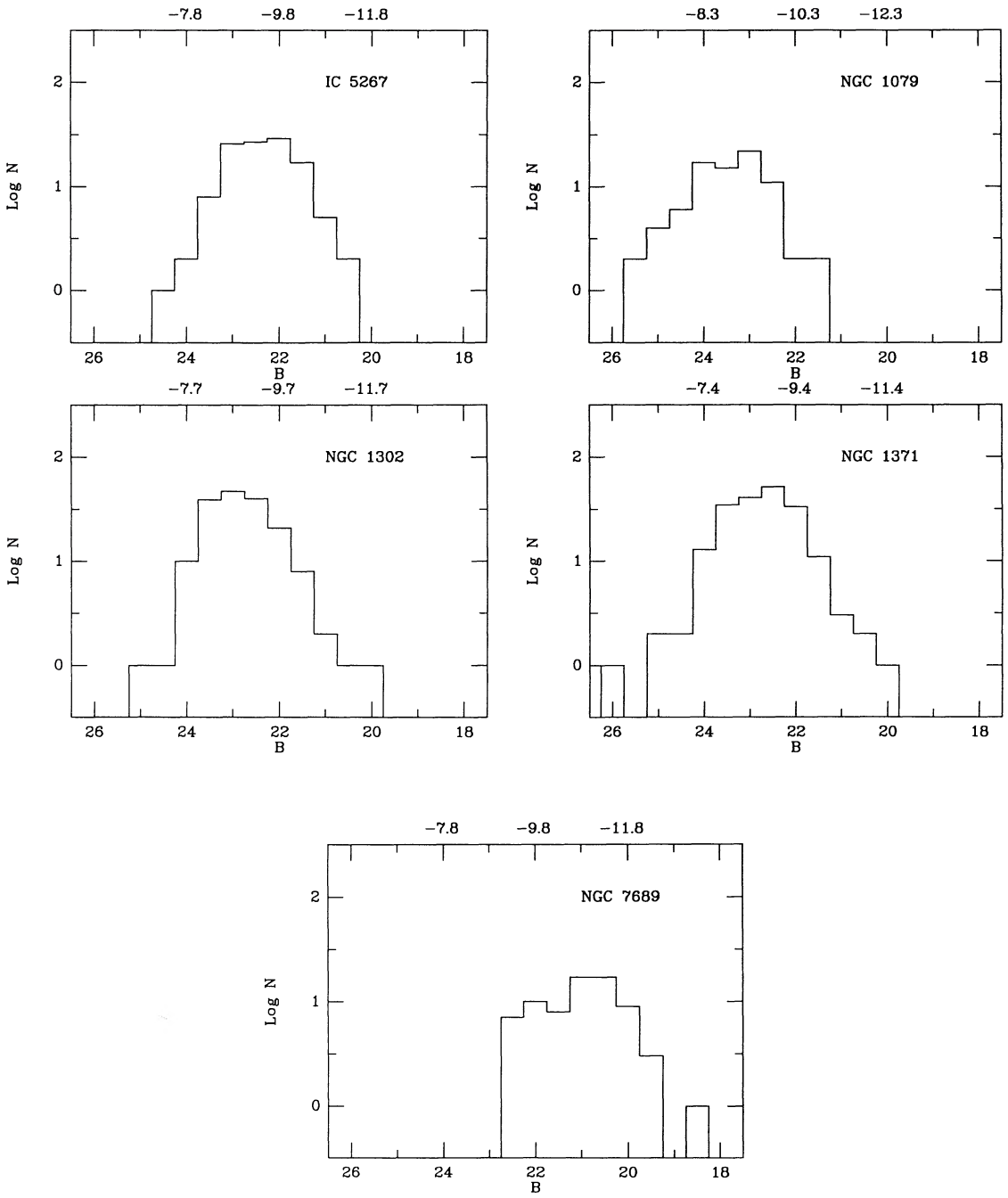

FIG. 12.—*B* luminosity functions for the knots. The bin size is 0.5 mag. Absolute magnitude scales as in Fig. 11.

5. STAR FORMATION RATES

5.1. *Total* Hα *Luminosities*

To calculate the global star formation rate, we need to know the global Hα luminosity. There are two ways to calculate that quantity. First, we can simply add up the measured luminosities of the individual H II regions reported earlier. KEH have presented evidence, however, that occasionally galaxies have a large fraction of their total Hα emission in a diffuse form, not associated with bright H II regions, and therefore not measured when individual regions are measured. The effect, they believed, became greater for earlier type spirals. We chose to compute the global Hα using two methods, one involving the measurements of the individual regions and one that adds up all of the Hα emission regardless of its location. To do the latter, we added up all of the sky-subtracted Fabry-Perot CCD frames, and then subtracted from that sum a scaled continuum frame, itself often the average of two frames. The nuclear area and any foreground stars were masked off (none of the galaxies clearly had any significant nuclear emission), as were regions that were obviously blank sky or devoid of emission. The remaining pixels were added up, and the intensity value was

© American Astronomical Society • Provided by the NASA Astrophysics Data System

1991ApJ...370..526C

transformed into a Hα luminosity as before. This technique is very sensitive to the assumed sky value, and errors of up to 20% are to be expected. The values are listed in Table 2, along with the sum of the individual regions. Some of the Sa galaxies indeed do appear to have substantial diffuse ionized gas, but for the others (e.g., NGC 7410) there is little evidence for it. The Sc also has little unaccounted-for ionized gas, as would have been predicted by KEH. We will calculate star formation rates below using only the Hα measured in discrete regions, since there is little difference in the mean between those values and the global Hα.

5.2. *Rates*

To calculate the current star formation rates, we used the methodology employed in Kennicutt (1983), in which case B recombination theory, an assumed IMF, and stellar evolution tracks allowed a conversion from Hα photons to star formation rate to be made. The assumed IMF is that for late-type spirals by Kennicutt (1983). It is essential to bear in mind that if the form of the IMF at the low-mass end varies significantly as a function of Hubble type, the comparisons made here will be affected accordingly. Our use of a different distance scale requires some modifications to the numbers published in the earlier work, which used $H_0 = 50$ and assumed a uniform Hubble flow. We also want to point out that the current star formation rate as calculated here depends on H_0^{-2}, the past rate on H_0^{-1} (because of the use of M/L), and the ratio on H_0^{-1}. The current rate per unit area and the gas depletion times discussed below are distance-independent. The total Hα luminosity is the largest source of error in the calculated rates; probable errors are on the order of 20%–30%. The rates per unit area should be relatively more accurate, since we did not have to incorporate the fractional areas observed. The current rates are listed in Table 4.

The Sa galaxies have current star formation rates ranging from 0.06 to 0.4 $M_\odot$ yr^{-1}. This can be contrasted with the corrected rates for Sc galaxies (Kennicutt 1983), which range from 0.5 to 9 $M_\odot$ yr^{-1} and have a median value of 1.3, about 15 times higher than the median for the Sa's studied here. NGC 7689, our Sc, has a current rate of about 2 $M_\odot$ yr^{-1}, while, as expected, the Sab galaxy NGC 1398 has an intermediate rate at 0.8 $M_\odot$ yr^{-1}. NGC 1079 is the weakest galaxy in terms of star-forming ability, making only 0.06 $M_\odot$ pc^{-2} Gyr^{-1}, 60 times less prodigious than our own Galaxy. IC 5267 has the strongest star formation rate, 7 times higher than NGC 1079, illustrating the diversity among Sa's.

Average past star formation rates were found by taking the disk luminosities, multiplying by M/L_B, and dividing by the time elapsed since star formation began. The disk luminosities were derived from the CCD images, and the corresponding bulge/disk ratios are listed in Table 4. The bulge/disk ratio for NGC 4594 was taken from Burkhead (1986) and Kent (1988), while the table values that are in parentheses are guesses based on the sky survey plates. Our bulge/disk values fall within the range of values found for a different set of Sa's by Kent (1988). In principle, we can actually derive the individual M/L_B's, since we have velocity information for each galaxy, but we leave that for the future and for the moment refer to the M/L_B's tabulated in Faber & Gallagher (1979). As in Kennicutt (1983), we correct the Faber and Gallagher M/L_B's for a Galactic extinction model with no absorption at the Galactic poles, and use diameters measured at $B = 25$ mag arcsec^{-2}, since disk star formation seems to stop there, even for our Sa's. We further correct the M/L_B's to $H_0 = 75$, and wind up with a value of 4.8 for Sa galaxies. Van Driel (1987) measured H I rotation velocities for IC 5267, which, when combined with our photometry, gives $M/L_B = 6.5$, close to what we assumed for all of the Sa's. The average past star formation rate for that galaxy calculated with van Driel's data is also in good agreement with the value calculated using the average M/L_B value. To maintain agreement with the Kennicutt (1983) rates, we assume that star formation began 15 Gyr ago, roughly consistent with our value for H_0. The past rates are also listed in Table 4, as are the ratios of present to past. Values for the Sc's done by Kennicutt (1983) as well as for the Galaxy (Tinsley 1980) are also listed.

The strongest distinction between early- and late-type disk galaxies lies in the star formation history: current star formation in Sa galaxies is of the order of 1% of the average past rate, while the star formation in Sc galaxies proceeds at a rate comparable to that which has always existed.

6. DISCUSSION

While we cannot rule out an Sa IMF with a slope somewhat different from that found in later type galaxies, we have positively shown that stars as massive as 10 $M_\odot$ exist, and have circumstantial evidence that many Sa's have stars as massive as those found in our own Galaxy. The *sizes* of star formation regions in Sa's are significantly different from those in later type galaxies. There are both fewer regions at all luminosities and no very luminous regions brighter than 10^{39} ergs s^{-1} whatsoever.

TABLE 4

STAR FORMATION RATES

Galaxy	Bulge/Disk Ratio	Current Rate ($M_\odot$ pc^{-2} Gyr^{-1})	Current Rate ($M_\odot$ yr^{-1})	Past Rate ($M_\odot$ yr^{-1})	Ratio	Depletion Time (yr)
NGC 1079	(0.5)	0.06	0.1	3.7	0.03	1.9×10^{11}
NGC 1291	(0.5)	0.1	0.09	5.7	0.02	5.0×10^{10}
NGC 1302	0.5	0.2	0.1	4.6	0.03	3.2×10^{10}
NGC 1371	0.5	0.3	0.3	3.0	0.1	4.8×10^{10}
NGC 1398	(0.4)	0.7	0.8	8.1	0.1	1.2×10^{10}
NGC 4594	6.0	0.2	0.08	5.0	0.02	2.0×10^{10}
NGC 7410	(0.5)	0.1	0.06	5.2	0.01	$< 1.9 \times 10^{10}$
IC 5267	0.4	0.4	0.4	5.1	0.08	2.7×10^{10}
NGC 7689	(0.0)	4.7	2.2	2.6	0.85	4.8×10^{9}
MW	(0.0)	4.0	5.0	5.0	1.00	3.0×10^{9}
Sc's	(0.0)	4–20	1–5	...	0.3–0.7	$2–8 \times 10^{9}$

© American Astronomical Society • Provided by the NASA Astrophysics Data System

1991ApJ...370..526C

Why is this so? We believe that the difference in the character of star formation in Sa's can be explained by the fact that the local gas density throughout the disks is below the threshold surface gas densities defined by

$$\Sigma_c = \alpha\kappa c/\pi G ,$$

where κ is the epicyclic frequency, c is the velocity dispersion of the gas, and $\alpha = 0.7$ for late-type galaxies (Kennicutt 1989). In regions where the surface gas density is higher than the threshold density, star formation obeys a power-law relation with the local gas density and is a global phenomenon, that is, it occurs everywhere. Such is the case for the late-type galaxy disks, except at the large radii. The gas within those regions is unstable to gravitational collapse, and hence to star formation. Star formation is not found at gas densities well below the threshold. At surface gas densities near the threshold density, star formation does occur but is not global, and is probably due to local effects, such as the passage of density waves or isolated density enhancements due to supernova explosions or perhaps simply leftovers from a more dynamic past. Such is the case obtained at large radii in Sc's and the Sab's and some Sb's studied by Kennicutt (1989).

The H I and velocity field of IC 5267 have been mapped by van Driel (1987), which allows us to apply the threshold ideas to an Sa galaxy. Van Driel found that the H I surface density was nowhere higher than 1.9 $M_\odot$ pc^{-2}. Figure 13 (adapted from Kennicutt 1989) shows the run of gas surface density over the local critical density as a function of radius in IC 5267. A horizontal line indicates the critical level found in late-type galaxies. IC 5267 is everywhere below that critical level. The gas in that galaxy is stable against spontaneous gravitational collapse, yet star formation is widespread. The total gas content of the other Sa's is similar to or lower than that in IC 5267, so it would appear to be safe to assume that the gas densities in those galaxies are as low as in IC 5267, although it would clearly be preferable to have H I and CO maps of these galaxies. These Sa galaxies are probably below but near the threshold densities, and thus star formation must have been induced by local phenomena and not by spontaneous gravitational collapse. Several of the Sa's have inner spiral arms, well defined by the H II regions, so in those cases the gas which would normally not have high enough densities to collapse is able to do so in the presence of a presumed density wave. Most of the star formation is, however, more flocculent and not discernibly in spiral arms. In summary, the very low levels of star formation in Sa's can be explained by the fact that the gas densities are everywhere below the critical value for spontaneous gravitational collapse; thus star formation is much more inhibited in Sa's with respect to later type galaxies than would be predicted by a simple power-law dependence of star formation rate on gas density.

Why the star formation history in Sa's is so different from that of later type galaxies is a perplexing question. While the past rates are only integral values, for late types it would seen to be artificial to say that the past rate of star formation in the disks was in fact not constant, but that things conspired over time to make the average rate equal to the current rate. That possibility seems even more unlikely when we consider that we do know that the Milky Way has maintained a rate within a factor of 2 of the current rate over the lifetime of the disk (Twarog 1980). For the Sa's, however, we cannot be sure what went on in the past, at least until we are able to look into the past with better resolution. Three results of this paper are the following: (1) the current star formation rate is of the order of 1% of the average past rate, (2) the average past rate is of the order of the average past rate of late-type galaxies, and (3) current star formation is in the threshold regime. Two possible extremes of histories which would be consistent with those results are (*a*) that the star formation rate did not greatly change over time until the gas densities reached the threshold density or, alternatively, (*b*) that the star formation rate was rapid at some time(s) but declined steeply thereafter.

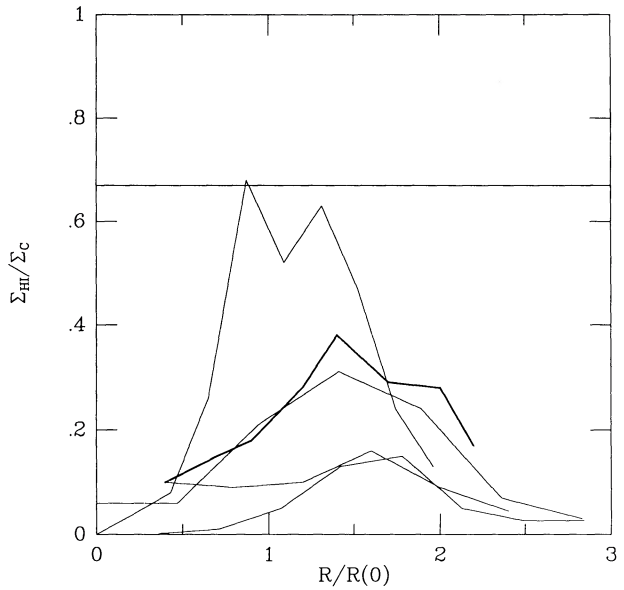

FIG. 13.—The run of the ratio of local gas density to the threshold density as a function of radius [normalized to $R(0)$], for a number of S0's and IC 5267 (*heavy line*). The horizontal line is the ratio where star formation in late-type galaxies is markedly curtailed.

If alternative *a* is the case, the rate was constant at the value found in late-type galaxies up until the point when the gas density dropped below the threshold density, and the reason for the differences in present-day morphology among galaxies must be that the amount of gas originally doled out to them was different. Sa's used up their gas earlier only because they did not have as much to begin with, not because they had faster rates. This scheme of galaxy formation may seem similar to that proposed earlier by Sandage, Freeman, & Stokes (1970), but in detail it is quite different in that our new data require substantial changes in galaxy morphology after the gas density dropped below the threshold level, probably within the last few billion years. The question of why less gas was initially available to some galaxies is probably related to the formation of the bulges in those Sa galaxies that have prominent ones, and is probably related to the subsequent history of interactions for small-bulge Sa's.

Alternative *b* requires even stronger changes in star formation morphology, though they could have occurred much longer ago, resulting in a star formation rate over time near that found in the steadier Sc's. An era of rapid star formation could have been prompted by numerous interactions, such as might have been required to make the large bulges, and/or simply be due to a high power dependence of the rate on gas density. The rapid star formation would have depleted the

© American Astronomical Society • Provided by the NASA Astrophysics Data System

1991ApJ...370..526C

available gas to the threshold density quicker than in later type galaxies.

For either scenario or modifications thereof, it would seem logical to conclude that the star formation in the disks of Sa's when the rate was much higher had the character we see in the later type galaxies at current epochs, that is, many star formation sites at all luminosities, as well as huge complexes not seen in present-day Sa's. Blue cluster galaxies at $z \gtrsim 0.2$ have spectra that have been interpreted to be the result of a fairly high rate of star formation that was abruptly diminished (Butcher & Oemler 1978, 1984; Dressler & Gunn 1983; Couch & Sharples 1987; Newberry, Boroson, & Kirshner 1990). The specific effect may have been either a burst or the cessation of star formation in a "late-type galaxy" which had a relatively high star formation rate to begin with. Perhaps in some cases this effect represents the onset of the epoch of low star formation rate in galaxies that would become Sa or earlier type disk galaxies, with rates that are so low as to be easily mistaken for zero in low signal-to-noise spectra.

Many of the galaxies observed in this project have aperture synthesis or single-dish measurements of their H I masses, and therefore we can calculate gas depletion times by star formation. We divide the gas mass by the star formation rate, and correct for the amount of gas returned to the interstellar medium by dying stars. As we have shown, there is no good reason to believe that the high-mass end of the IMF in Sa's is different from that in late-type galaxies, and so we assume a return fraction that is applicable for a normal IMF of 25%. For IC 5267, the H I gas mass measured by van Driel (1987) is $3.09 \times 10^9\ M_\odot$, which we correct first to our assumed distance of 22.4 Mpc, second for the presence of helium and molecular gas by multiplying by 2, and finally for recycling by multiplying by 1.25. The depletion time is then 2.7×10^{10} yr. For NGC 4594, Faber et al. (1977) have measured an H I mass of $8.7 \times 10^8\ M_\odot$. Correcting the mass as before, and dividing by the galaxy's current star formation rate, we get a depletion time of 2.0×10^{10} yr. Other H I measurements can be found in the compilation of Huchtmeier & Richter (1989) and, when corrected as above, also lead to depletion times greater than 10^{10} yr, as can be seen in the last column of Table 4. These numbers are unusually large; few of the galaxies studied in Kennicutt (1983) have such large times. Those that do are Sc's, mostly low-luminosity, and one can only speculate that these have large H I halos that extend well beyond the area of star formation in the disks.

From a study of star formation in galaxies of all types, as predicted by the flux at $\sim$2000 Å, Donas et al (1987) reported a slight increase in the depletion times for later Hubble types, in contrast to the effect we report here. The particular disagreement with out result is in the depletion times for Sa's (type 1 in their paper), for which they apparently get an average depletion time of 2.5×10^9 yr, when corrections for molecular gas content and recycling of gas are applied as we have done here. However, only one galaxy in their sample is classified as an Sa in the RSA; most of the others called type 1 in the SRC are fainter galaxies, and hence have more uncertain classifications. The one Sa in the Donas et al. study has a depletion time of 1.5×10^{10} yr, similar to the values reported here.

Young & Knezek (1989) have suggested that the H_2/H I ratio changes as a function of Hubble type, from about 4 to 0.7 in the range of S0/Sa to Sc. Such a change would make the differences in depletion times in that morphological range even more extreme. A change in the low-mass end of the IMF along the Hubble sequence (such that the early types make relatively more low-mass stars) would affect our results, but the change required is large, and becomes absurd when we consider that yet lower star formation rates may exist in galaxies with the same total gas mass as those we have studied here.

It seems unlikely that the Sa depletion times are exact; surely star formation will stop once the densities fall to a tenth of their present value, but even that time is several Gyr in the future. The Sa depletion times, however, do tell us that the late-type galaxy depletion times are definitely not to be taken at face value. It seems more likely that the depletion times in the latter galaxies mark off time until the character of star formation changes, once the gas densities approach those measured in the Sa's, that is, below the thresholds described in Kennicutt (1989). At that time for each galaxy, the star formation rate will drop precipitously. Large complexes of star formation will disappear, to be replaced by the small sites similar to those found now in Sa's, and the total number of sites will be cut drastically. Because of the lowered star formation rate, the depletion times will be extended beyond the nominal 5 Gyr time, perhaps by only a few more Gyr, but possibly by as much as 10 Gyr. Star formation in the universe will most likely continue for as long in the future as it has existed already.

REFERENCES

Bucknell, M. J., & Peach, J. V. 1976, Observatory, 96, 61
Burkhead, M. S. 1986, AJ, 91, 777
Butcher, H., & Oemler, A. 1978, ApJ, 219, 18
———. 1984, ApJ, 285, 426
Caldwell, N., & Phillips, M. M. 1989, ApJ, 338, 789
Couch, W. J., & Sharples, R. M. 1987, MNRAS, 229, 423
Donas, J., Deharveng, J. M., Laget, M., Milliard, B., & Huguenin, D. 1987, A&A, 180, 12
Dressler, A., & Gunn, J. E. 1983, ApJ, 270, 7
Faber, S., Balick, B., Gallagher, J., & Knapp, G. 1977, AJ, 214, 383
Faber, S., & Gallagher, J. 1979, ARA&A, 17, 135
Graham, J. A. 1981, PASP, 95, 552
Hodge, P., & Kennicutt, R. 1983, AJ, 88, 296
Hubble, E. 1936, The Realm of the Nebulae (New Haven: Yale Univ. Press)
Huchtmeier, W. K., & Richter, O.-G. 1989, A General Catalogue of H I Observations of Galaxies (New York: Springer-Verlag)
Hunter, D. A., & Massey, P. M. 1990, AJ, 99, 846
Kennicutt, R. C. 1983, ApJ, 272, 54
———. 1988, ApJ, 334, 144
———. 1989, ApJ, 344, 685
Kennicutt, R. C., Edgar, K., & Hodge, P. 1989, ApJ, 337, 761 (KEH)
Kent, S. 1988, AJ, 96, 514
Kormendy, J. 1977, in The Evolution of Galaxies and Stellar Populations, ed. B. M. Tinsley & R. B. Larson (New Haven: Yale Univ. Obs), 131
Larson, R., & Tinsley, B. M. 1978, ApJ, 219, 46
Lundmark, K. 1926, Ark. Mat., Astr. och Fys., 8, 19b
Newberry, M. V., Boroson, T. A., & Kirshner, R. P. 1990, ApJ, 350, 585
Sandage, A., Freeman, K. C., & Stokes, N. R. 1970, ApJ, 160, 831
Sandage, A., & Tammann, G. 1974, ApJ, 194, 223
———. 1987, A Revised Shapley-Ames Catalog of Bright Galaxies (Washington, DC: Carnegie Inst. Washington Pub. 635) (RSA)
Schommer, R., Caldwell, N., Wilson, A. S., Baldwin, J. A., Phillips, M. M., Williams, T. B., & Turtle, A. J. 1988, ApJ, 324, 154
Schweizer, F. 1978, ApJ, 220, 98
Searle, L., Sargent, W. L. W., & Bagnuolo. W. G. 1973, ApJ, 179, 427
Tinsley, B. M. 1980, Fund. Cosmic Phys. 5, 287
Twarog, B. 1980, ApJ 242, 242
van den Bergh, S. 1976, AJ, 81, 797
van Driel, W. 1987, Ph.D. thesis, University of Groningen
Young, J. S., & Knezek, P. M. 1989, ApJ, 347, L55

© American Astronomical Society • Provided by the NASA Astrophysics Data System